

MODELING AN INPUT-OUTPUT GEOKINETIC SYSTEM
UTILIZING A FINITE ELEMENT APPROACH

Robert Charles Foos

Library
Naval Postgraduate School
Monterey, California 93946

NAVAL POSTGRADUATE SCHOOL

Monterey, California



THESIS

MODELING AN INPUT-OUTPUT GEOKINETIC SYSTEM
UTILIZING A FINITE ELEMENT APPROACH

by

Robert Charles Foos

March 1975

Thesis Advisors:

Donald R. Barr
Rex H. Shudde

Approved for public release; distribution unlimited.

T168187

UNCLASSIFIED

SECURITY CLASSIFICATION OF THIS PAGE (When Data Entered)

REPORT DOCUMENTATION PAGE		READ INSTRUCTIONS BEFORE COMPLETING FORM
1. REPORT NUMBER	2. GOVT ACCESSION NO.	3. RECIPIENT'S CATALOG NUMBER
4. TITLE (and Subtitle) Modeling an Input-Output Geokinetic System Utilizing a Finite Element Approach		5. TYPE OF REPORT & PERIOD COVERED Master's Thesis; March 1975
		6. PERFORMING ORG. REPORT NUMBER
7. AUTHOR(s) Robert Charles Foos		8. CONTRACT OR GRANT NUMBER(s)
9. PERFORMING ORGANIZATION NAME AND ADDRESS Naval Postgraduate School Monterey, California 93940		10. PROGRAM ELEMENT, PROJECT, TASK AREA & WORK UNIT NUMBERS
11. CONTROLLING OFFICE NAME AND ADDRESS Naval Postgraduate School Monterey, California 93940		12. REPORT DATE March 1975
		13. NUMBER OF PAGES
14. MONITORING AGENCY NAME & ADDRESS (if different from Controlling Office) Naval Postgraduate School Monterey, California 93940		15. SECURITY CLASS. (of this report) Unclassified
		15a. DECLASSIFICATION/DOWNGRADING SCHEDULE
16. DISTRIBUTION STATEMENT (of this Report) Approved for public release; distribution unlimited.		
17. DISTRIBUTION STATEMENT (of the abstract entered in Block 20, if different from Report)		
18. SUPPLEMENTARY NOTES		
19. KEY WORDS (Continue on reverse side if necessary and identify by block number) Finite Element Earth Surface Tilt Tidal Ocean Loading Geokinetics		
20. ABSTRACT (Continue on reverse side if necessary and identify by block number) The modeling research presented in this paper of an input-output geokinetic system can be applied to problems not only in earthquake research but also to problems in siloed missile systems. The finite element technique provides an effective methodology for exploring the detailed surface movements of the earth in response to ocean tidal loading. The finite element computer program utilized in this paper was especially designed		

DD FORM 1 JAN 73 1473
(Page 1)EDITION OF 1 NOV 65 IS OBSOLETE
S/N 0102-014-6601UNCLASSIFIED
SECURITY CLASSIFICATION OF THIS PAGE (When Data Entered)

UNCLASSIFIED

SECURITY CLASSIFICATION OF THIS PAGE(When Data Entered)

for analyzing deformations and strains resulting from a system of loads applied to a structure. Relationships are explored between surface loads and fault zone tilt response as a function of fault zone shear strength, and distance of the fault from the load.

UNCLASSIFIED

SECURITY CLASSIFICATION OF THIS PAGE(When Data Entered)

Modeling an Input-Output Geokinetic System
Utilizing a Finite Element Approach

by

Robert Charles Foos
Captain, United States Army
B.S., United States Military Academy, 1969

Submitted in partial fulfillment of the
requirements for the degree of

MASTER OF SCIENCE IN OPERATIONS RESEARCH

ABSTRACT

The modeling research presented in this paper of an input-output geokinetic system can be applied to problems not only in earthquake research but also to problems in siloed missile systems. The finite element technique provides an effective methodology for exploring the detailed surface movements of the earth in response to ocean tidal loading. The finite element computer program utilized in this paper was especially designed for analyzing deformations and strains resulting from a system of loads applied to a structure. Relationships are explored between surface loads and fault zone tilt response as a function of fault zone shear strength, and distance of the fault from the load.

TABLE OF CONTENTS

I.	INTRODUCTION-----	8
II.	FINITE ELEMENT MODEL CONTRASTED WITH BOUSSINESQ MODEL-----	11
III.	DEVELOPMENT OF RELATIONSHIPS BETWEEN FAULT ZONE TILT, FAULT LOCATION, FAULT SHEAR STRENGTH AND SURFACE LOADS-----	15
IV.	MODELS OF FOUR PROFILES OF THE CALIFORNIA COASTLINE-----	31
V.	AREAS FOR FURTHER STUDY-----	38
VI.	CONCLUSIONS-----	39
APPENDIX A	- DOCUMENTATION OF THE FINITE ELEMENT COMPUTER PROGRAM-----	40
APPENDIX B	- LISTING OF FINITE ELEMENT TECHNIQUE COMPUTER PROGRAM-----	57
BIBLIOGRAPHY	-----	77
INITIAL DISTRIBUTION LIST	-----	79

LIST OF TABLES

TABLE I	19
TABLE II	20
TABLE III	24

LIST OF FIGURES

1.	FINITE ELEMENT STRUCTURE AND LOAD-----	12
2.	LOCATION MAP OF U.S. GEOLOGICAL SURVEY SEISMOGRAPH STATIONS AND MAJOR FAULTS IN CENTRAL CALIFORNIA-----	18
3.	FAULT ZONE TILT, SOFT BOTTOM MODEL-----	20
4.	FAULT ZONE TILT, HARD BOTTOM MODEL-----	21
5.	FAULT ZONE TILT, STEWART MODEL-----	22
6.	FAULT ZONE SHEAR MODULUS, SOFT BOTTOM MODEL-----	26
7.	FAULT ZONE SHEAR MODULUS, HARD BOTTOM MODEL-----	27
8.	FAULT ZONE SHEAR MODULUS, STEWART MODEL-----	28
9.	FIGURE OF DISPLACEMENT FIELD IN THE HARD BOTTOM MODEL-----	30
10.	FOUR CALIFORNIA PROFILES-----	53
11.	PROFILE A-----	34
12.	PROFILE B-----	35
13.	PROFILE C-----	36
14.	PROFILE D-----	37
15.	FIVE MESH TYPES-----	42
16.	SAMPLE OF COMPLETED GRID DESIGN-----	45

I. INTRODUCTION

This study explores modeling a specific input-output system in the field of geokinetics. A finite element technique is utilized as the system simulator. The Earth's surface movements are the output to several geophysical phenomena. One of the most significant geophysical inputs is ocean tital loading. Finite element modeling provides an effective technique for exploring the detailed surface movements of the earth in response to ocean loading.

The first chapter of this paper discusses the bounds of the finite element model. The finite element model is contrasted with an analytical half space Boussinesq technique in order to provide the level of detail which should be included in the finite element model. Tilts resulting from two and three dimensional surface loads on the Boussinesq half space models bracket the tilt produced by the two dimensional finite element model. In the second chapter relationships are explored between surface loads and fault zone tilt response as a function of fault zone shear strength, and distance of the fault from the load. The results indicate a logarithmic relationship between the magnitude of fault zone tilt and distance of the fault from the load. The final chapter describes four profiles of the California coastline in an attempt to relate real data collected by the United States Geological Survey to model results.

It is assumed that the reader is already familiar with solving families of differential equations by finite difference techniques and their applications to geophysical sciences. Only token consideration is given in this paper to the theory of finite difference techniques and their application to finite element modeling. The reader unfamiliar with finite element methodology is encouraged to read the appendix of this paper containing the documentation of the finite element computer program. This documentation should give the reader a better perception of the finite element modeling technique. There are also several excellent references published on the subject of finite element techniques [1, 9, 15].

There are many applications of the finite element technique besides solving geophysically related systems. The pure research which is presented in this paper can be applied to problems not only in earthquake research but, for example, also in air defense missile systems [2]. Accurately predicted ground motion near siloed missiles can be programmed into the missile's prelaunch parameters of the inertial guidance system. This information results in fewer course corrections required for the missile and therefore a higher probability of hitting its target.

The finite element computer program utilized in this paper was especially designed for analyzing deformations and strains resulting from a system of loads applied to a structure. This two dimensional finite element computer program was developed at the National Center for Earthquake Research of the United

States Geological Survey by Dr. James H. Dieterich [3], Dr. M. Darroll Wood and refined by the author. The author is greatly indebted to Dr. M. Darroll Wood for his cooperation, guidance and geophysics expertise which made this paper possible. The terminology and notation used in this paper was adopted from Dr. Wood's doctoral thesis [12]. The author also expresses his appreciation to Professor Donald Barr and Professor Rex Shudde for their helpful criticism and ideas during the stages of development of this paper. The William R. Church Computer Center was a tremendous asset in the cooperation and service which it provided in processing the finite element computer programs.

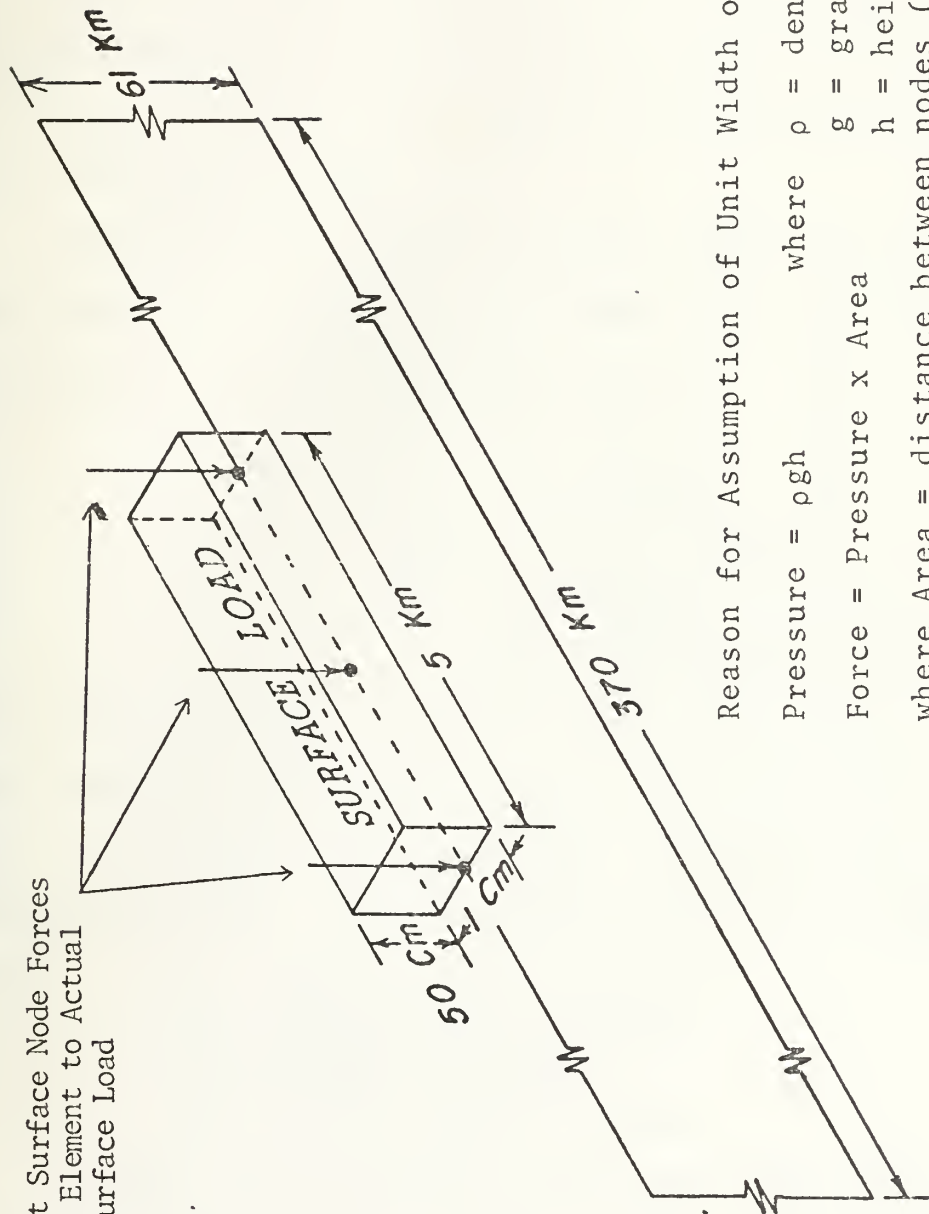
II. FINITE ELEMENT MODEL CONTRASTED WITH BOUSSINESQ MODEL

In 1878, Boussinesq calculated the vertical deviation of an elastic plane surface of a homogeneous medium under the loading effect caused by water. He showed that the vertical displacement of the Earth's crust was proportional at each point to the gravitational potential of the load and was a function of the elastic constants of the medium [8]. The Boussinesq technique has long been used as a simple approximation of load tilt. Load tilt is principally the gradient of the displacement field of the Earth's surface and two other secondary effects. The principal effect and the one which the finite element model simulates is that of the variable flexure of the Earth's crust under the loading effect caused by the oceans. The other effects are the attraction of the masses of water causing a vertical displacement of the Earth's surface, and the variation of the potential due to secondary deformation of the Earth's crust, an effect which is opposite in direction to the first and second effects [8].

The finite element structure is a two dimensional model in which the load is assumed to have unit width (Fig. 1). For this reason, it is difficult to directly compare the finite element model with Boussinesq half space models. The tilts calculated from the Boussinesq technique bounded the tilt produced from the finite element model in each of six

Finite Element Structure and Load

Equivalent Surface Node Forces
of Finite Element to Actual
Uniform Surface Load



Reason for Assumption of Unit Width of Surface Load

Pressure = ρgh where ρ = density of water

Force = Pressure x Area g = gravity

where Area = distance between nodes (length of

load) multiplied by a unit depth.

FIGURE 1

cases processed with different loads and elastic parameters. The finite element model overestimated the tilt calculated from the equivalent Boussinesq model with a two dimensional load, and consistently underestimated the tilt calculated from the equivalent Boussinesq model with a three dimensional load. The following description is of one model processed by the finite element model and the calculations associated with the Boussinesq method.

The Boussinesq method describes load tilt δ_x^l as the deviation of the vertical $\delta_x^a(r)$ due to a load of radial extent r multiplied by the Boussinesq factor m . Thus:

$$\delta_x^l = \delta_x^a(r) \cdot m \text{ where } m = \frac{\lambda + 2\mu}{4\pi(\lambda + \mu)\mu} \cdot \frac{g^2}{G}$$

where μ = shear modulus
 λ = modulus of rigidity (Lamé
 g = gravity Constants)
 G = gravitational constant.

The deviation of the vertical $\delta_x^a(r)$ due to a load of extent r and height h is the ratio of the horizontal gravity g_x to the vertical gravity attraction [12]. For the three dimensional Boussinesq model $\delta_x^a(r) = \frac{G \rho h}{g} \frac{d}{dx} \int \frac{dr}{r} = \frac{G \rho h}{g} \ln(r)$

where ρ = density of load (water)
 G = gravitational constant
 h = height of the load
 g = gravity (vertical)
 r = radial extent of load.

For the two dimensional Boussinesq model $\delta_x^a(r)$ is computed using a line integral. Thus, $\delta_x^a(r) = \frac{G \rho h}{g \cdot r}$ where ρ , G , h , g , r are the same as above [12].

The finite element model was programmed to use the same inputs as the Boussinesq models of a homogeneous medium

containing elastic parameters $\lambda = \mu = 6.2 \times 10^{11}$ dynes/cm² (Lamé constants).

To simulate the Boussinesq boundary conditions, the bottom edge of the finite element structural model was specified as rigid. The load was a symmetrical surface load of water one centimeter in height and five kilometers in length.

The tilt calculated at the load center of the finite element model was 3.85×10^{-10} radians. The three dimensional Boussinesq method produced a load tilt of 2.47×10^{-9} radians, and the two dimensional Boussinesq methods produced a load tilt of 3.77×10^{-16} radians.

Because of the consistency with which the finite element model was bracketed by the Boussinesq methods, it is presumed that the finite element program will be a useful tool for detailed analysis of deformations resulting from a variety of loads applied to inhomogeneous structures. In order to have continuity throughout this paper, the bottom edges of remaining finite element models were structurally designed rigid.

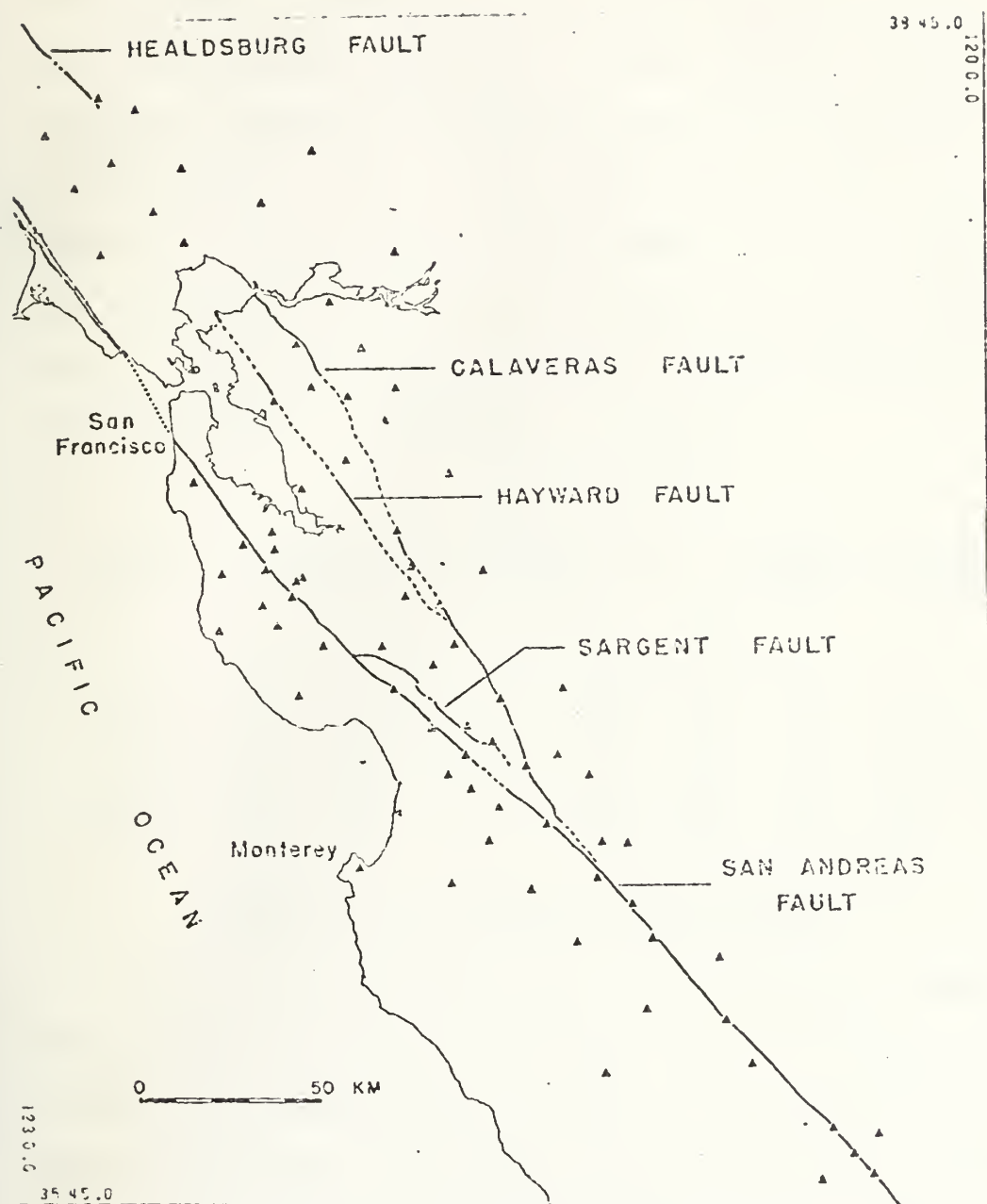
III. DEVELOPMENT OF RELATIONSHIPS BETWEEN FAULT ZONE TILT, FAULT LOCATION, FAULT SHEAR STRENGTH AND SURFACE LOADS

The response of earth structures to surface loads was explored utilizing the deterministic finite element model. The finite element model simulates the behavior of a discontinuous structure under asymmetric loading. The model structure was matched to the real Earth structure by laterally and vertically varying the known inhomogeneities of the earth. The response of the region near a vertical discontinuity, namely a fault, was of particular interest. The smallest homogeneous elements of the model were assumed to behave elastically for small increments of stress. However, the shear that is distributed in and near the fault zone elements or cells in the finite element grid may have varied considerably due to the contrast in Lamé constants for adjoining elements. The large difference in shear produces steps in the displacement field and therefore poses a problem of smoothness.

Tilt measurements in borehole and observatory sites have been made along the California coastline. Tilt measurements at tidal sensitivities (10^{-8} μ radians) show the Earth's surface response to oceanic loading is greater than responses from any other continuous source [13]. Conceivably, ocean loading constitutes a forcing function that can be used to derive the bulk elastic properties of the Earth. However, it has been shown that ocean tidal spectra are non-stationary

in all but lunar frequencies. The lunar semi-diurnal wave (M_2) is theoretically 85% of the energy of the total theoretical tidal spectrum [8]. In actuality this is not true. However, the M_2 line is sufficiently energetic and sufficiently removed from the contaminated tidal spectrum to be used as a stationary forcing function for earth response studies. For these reasons, the model surface load corresponded to the amplitude of the M_2 frequency. A value of fifty-three centimeters for the M_2 amplitude was chosen to represent the ocean loading in the central and northern California region [14]. In order to remain within the required aspect ratio in each cell of the finite element grid of 10:1 and to account for approximately 95% of the ocean loading effect as calculated by Boussinesq, the length of the load was chosen to be 165 kilometers [8]. With this loading, the investigation was limited to exploring relationships between fault zone tilt, fault shear strength, and the distance from the load to the fault. A factorial arrangement was developed by processing three slightly different velocity structure models having twelve fault locations and four fault shear moduli. The width and depth of the fault zone were set at five and sixteen kilometers respectively. These dimensions conform with Mayer-Rosa's [7] conclusion that the fault zone must be a low velocity zone at least several kilometers wide, extending into the lower crust. The fault zone was shifted consecutively in five kilometer increments from the edge of the load (coastline) to 60 kilometers inland.

This range of distances spans the extent of separation between the San Andreas Fault and the Pacific Ocean throughout most of central and northern California (Fig. 2). At each fault zone location, the shear strength of the fault was varied by adjusting the shear modulus in the fault zone. Starting with values of fault zone shear modulus set equal to adjacent elements, and then in consecutive models reducing the shear modulus in the fault zone one order of magnitude decrements, a maximum difference of four orders of magnitude less of shear strength in the fault zone was achieved.



Location map of U.S. Geological Survey seismograph stations and major faults in central California.

FIGURE 2

The Lamé constants computed for each cell were derived from studies of the seismic velocity models of Stewart [11] and the works he referenced. Three slightly different velocity structures were developed to observe differences in fault zone tilt response. The Poisson ratio was adjusted from 0.4 at the surface of the model to 0.25 at depths below ten kilometers. The density was derived using a Nafe-Drake curve. The three velocity models are represented by their associated elastic parameters in Table I.

TABLE I

DEPTH	HARD BOTTOM MODEL		SOFT BOTTOM MODEL		STEWART GABILAN MODEL		DIABLO MODEL	
	λ	μ	λ	μ	λ	μ	λ	μ
1.0	0.28	0.12	0.28	0.12	0.28	0.12	1.1	4.5
6.0	2.3	1.5	2.3	1.5	1.6	1.0	2.3	1.5
16.0	3.3	3.3	3.3	3.3	3.3	3.3	3.3	3.3
26.0	4.3	4.3	4.3	4.3	4.3	4.3	4.3	4.3
41.0	6.5	6.5	6.5	6.5	6.5	6.5	6.5	6.5
61.0	6.5	6.5	1.1	0.45	6.5	6.5	6.5	6.5

λ and μ are in units of 10^{11} dynes/cm².
 Depths are in units of kilometers.

Tilt was calculated as the maximum positive slope of displacement throughout each fault zone. The phase of tilt in which the displacement gradient is toward the load is taken as positive. By examining the results of the finite element model for these three velocity structures, a relationship between fault zone tilt and the distance from the load to the fault was hypothesized. The calculated tilt in the fault zone was plotted logarithmically against linear distance between the fault zone and the edge of the load (Fig. 3, 4, 5). For distances between 10 and 45 kilometers,

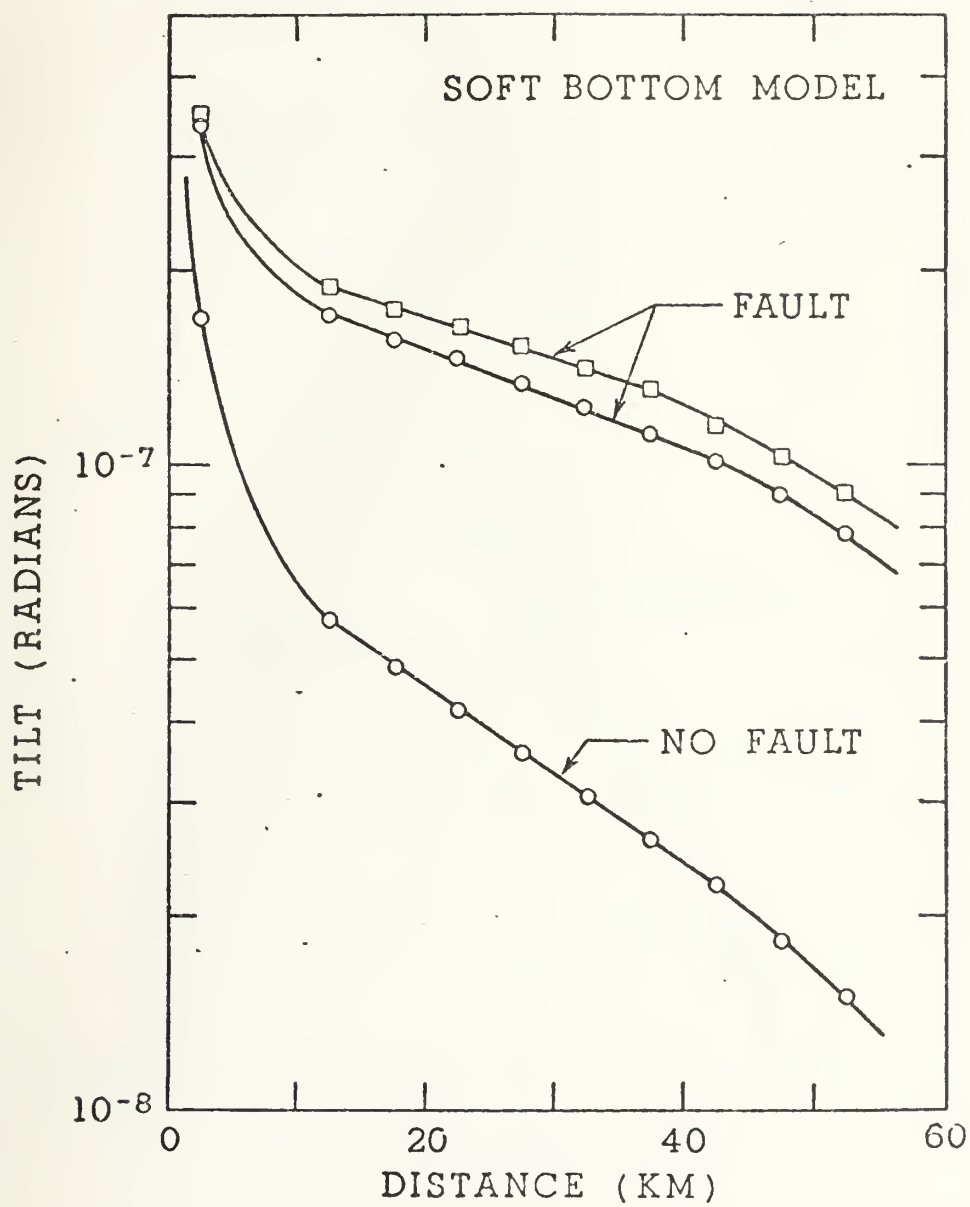


FIGURE 3

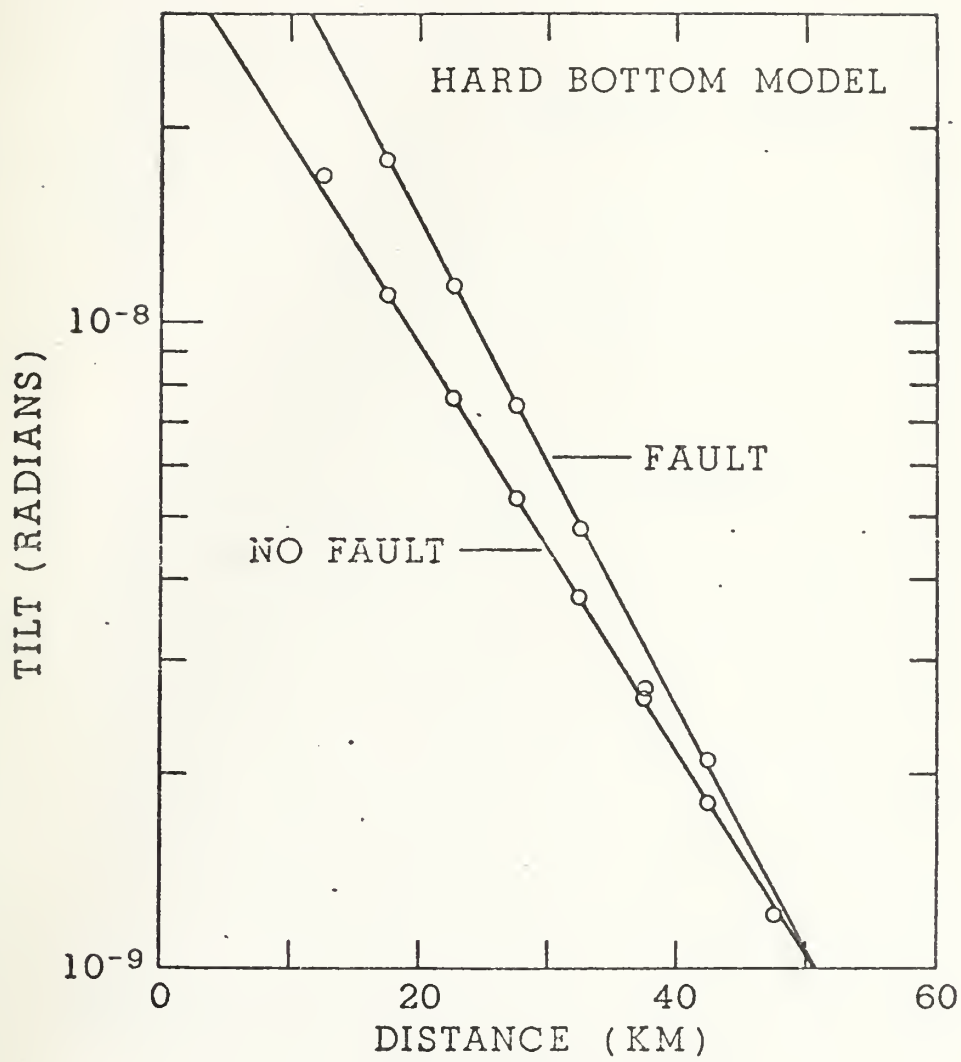


FIGURE 4

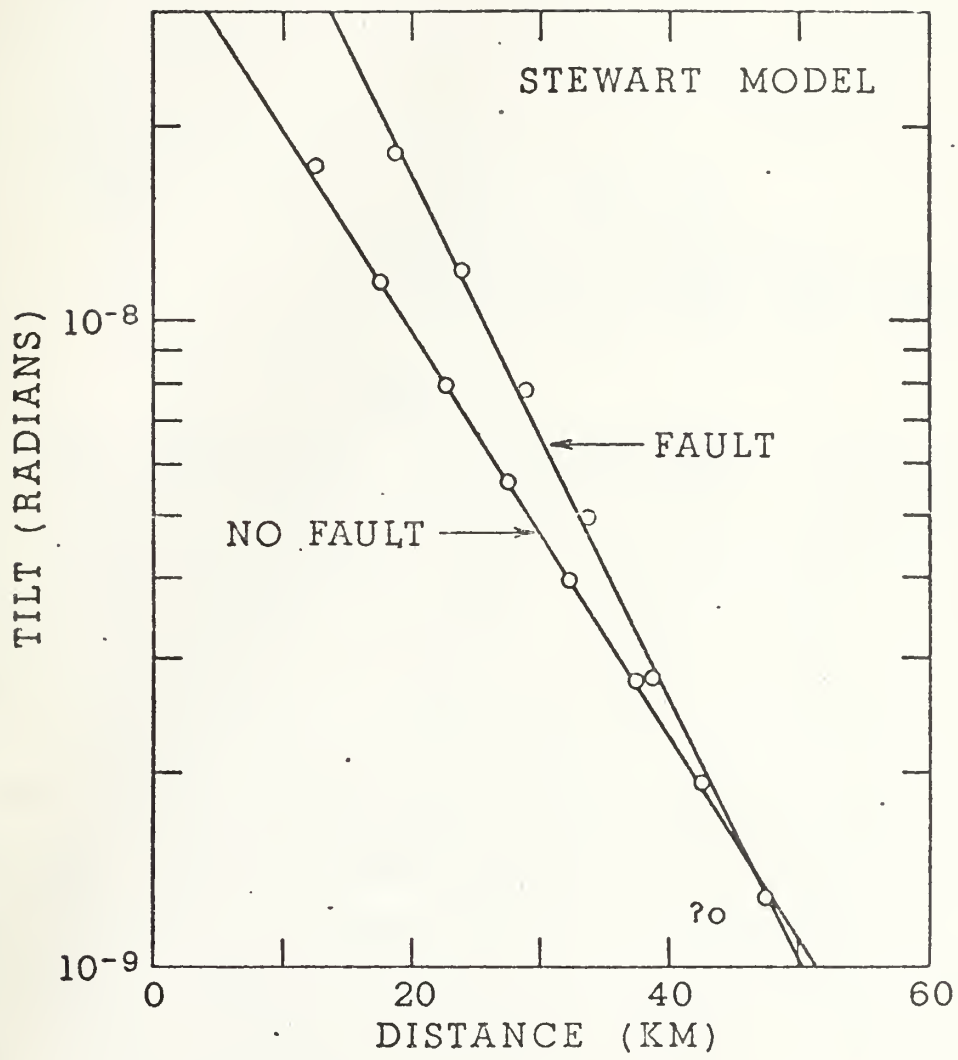


FIGURE 5

the tilt measurements lie nearly on a straight line for all three models and fault moduli. Straight lines on semi-logarithmic graph paper characterize the relationship as exponential. Equations describing the relationship between fault zone tilt and fault zone location are easily estimated from the graphs. The basic model is shown below, followed by Table II showing the value of each of the parameters for each velocity structure and fault shear strength.

$$T = T_0 e^{-s \cdot d}$$

where T = fault zone tilt
 T_0 = tilt intercept
 s = slope of straight line
 d = distance between fault zone and edge of the load (coastline)

TABLE II

	SOFT BOTTOM MODEL		HARD BOTTOM MODEL		STEWART MODEL	
	NO FAULT	FAULT	NO FAULT	FAULT	NO FAULT	FAULT
T_0	8.5×10^{-8}	2.15×10^{-7}	3.9×10^{-8}	8.0×10^{-8}	4.0×10^{-8}	1.1×10^{-7}
S	0.032	0.018	0.073	0.087	0.072	0.094
RANGE	5 < d < 50 km		10 < d < 50 km		10 < d < 45 km	

Tilt is strongly dependent on the shear modulus of the fault zone. When the shear modulus is decreased in the fault zone one order of magnitude from surrounding material, there is a distinct difference in the resulting tilt as compared with no fault structures. However, decreasing the shear modulus in the fault zone consecutively two, three and four orders of magnitude resulted in a small change of the fault zone tilt. This apparent convergence can best be seen from the table of calculated tilt in the fault zone for the three models (Table III). Plots of the shear modulus (μ) versus

TABLE III

FAULT ZONE	SOFT BOTTOM MODEL			HARD BOTTOM MODEL			STEWART MODEL				
	$\mu=10^9$			$\mu=10^8$			$\mu=10^9$				
	NO	FAULT	$\mu=10^7$	NO	FAULT	$\mu=10^7$	NO	FAULT	$\mu=10^8$	$\mu=10^7$	$\mu=10^6$
0-5	25.2	40.7	41.8	41.9	20.8	40.1	42.6	42.8	45.5	47.5	47.6
5-10	7.24	19.6	21.0	21.2	2.99	8.90	9.29	9.33	10.1	10.6	10.7
10-15	5.72	17.0	18.7	18.8	1.69	3.20	3.27	3.28	3.77	3.89	3.90
15-20	4.84	15.6	17.3	17.5	1.11	1.77	1.88	1.89	1.82	1.89	1.90
20-25	4.17	14.5	16.3	16.5	0.76	1.14	1.24	1.26	1.18	1.24	1.25
25-30	3.56	13.5	15.2	15.4	0.53	0.75	0.84	0.85	0.78	0.83	0.84
30-35	3.08	12.4	14.0	14.2	0.37	0.48	0.54	0.55	0.50	0.53	0.54
35-40	2.62	11.2	12.8	12.9	0.26	0.27	0.32	0.33	0.28	0.31	0.31
40-45	2.21	10.1	11.5	11.7	0.18	0.11	0.15	0.16	0.12	0.13	0.13
45-50	1.83	8.93	10.3	10.4	0.12	.004	0.02	0.03	*	.0004	.002
50-55	1.51	7.82	9.01	9.15	0.08	*	*	*	*	*	*
55-60	1.20	*	*	*	0.05	*	*	*	*	*	*

Table contains tilt calculated in each fault zone location of three velocity structure models.

Tilt units (10^{-8} radians).

Fault zone is the distance from the edge of the load to fault zone (kilometers).

* Phase of tilt vector inverted.

fault zone tilt for each of the fault zone locations and velocity structures are shown in figures 6, 7, 8.

The dotted line segments of the graphs are the interesting feature. This part of the graph depicts the relationship between a no fault structure and a structure containing a fault zone of shear modulus decreased by one order of magnitude from surrounding material. There appears to be no similarities in this portion of the graphs for different fault zone locations. The dotted line portion of the graphs are flatter at fault zone locations further away from the load. The inference is that the more distant the loads, the less sensitive the response to a local discontinuity. Also, greater depths are required to adequately model distant loads. If the dotted lines in the graph are approximated as straight lines, then an equation relating the shear modulus to fault zone tilt is given by

$$T = A \cdot U^{-n}, \text{ where } \begin{array}{l} T = \text{fault zone tilt} \\ A = \text{tilt intercept} \\ U = \text{shear modulus of fault zone} \\ n = \text{slope of the straight line.} \end{array}$$

However, further study into particular fault zone locations is required before this equation can be verified.

There are several shortcomings in the modeling which has been presented. First, the soft bottom model is not a realistic representation of the Earth's velocity structure. However, this model does show a sensitivity with which fault zone tilt varies with slight changes in the overall velocity structure. The soft bottom model also unmistakably has the characteristic exponential relationship between fault zone

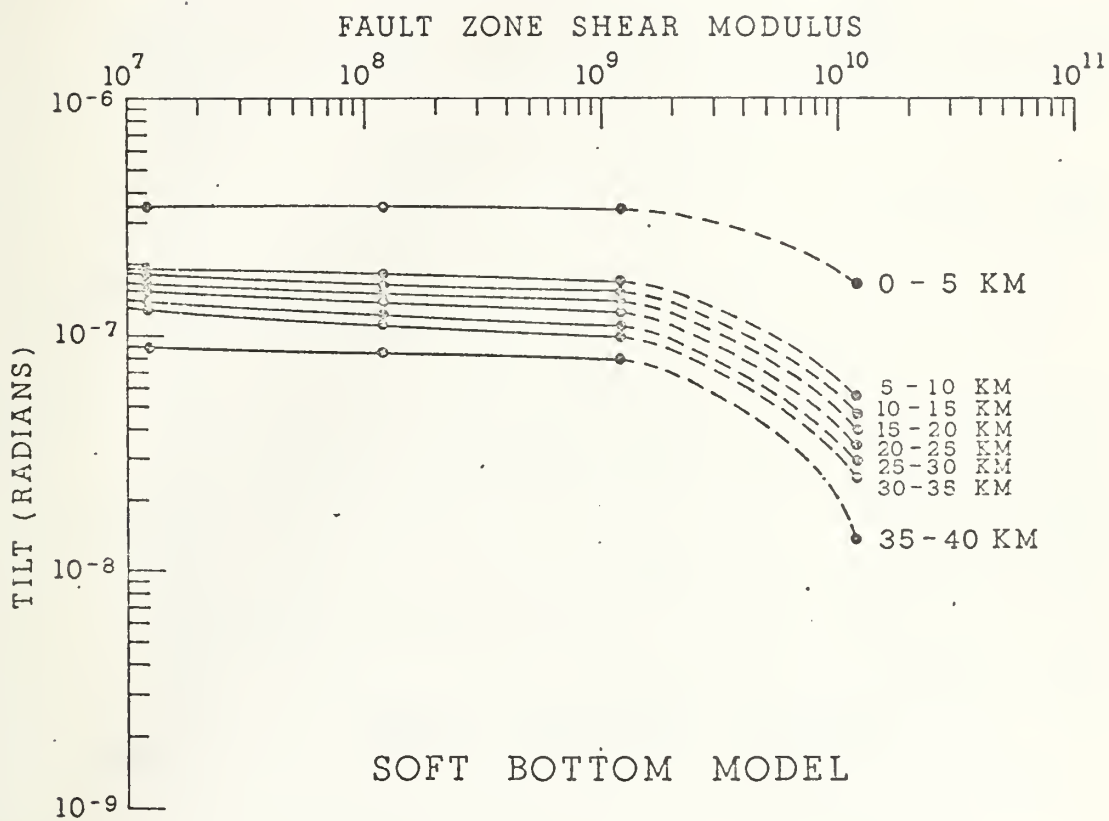


FIGURE 6

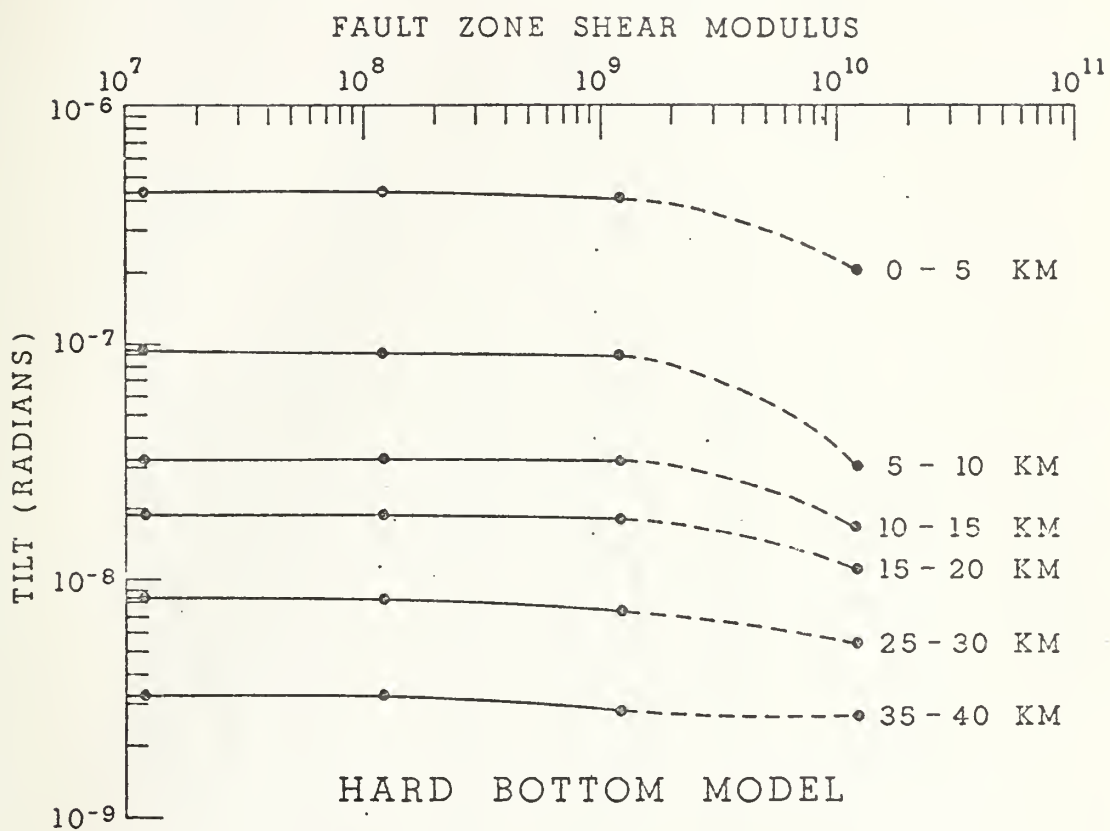


FIGURE 7

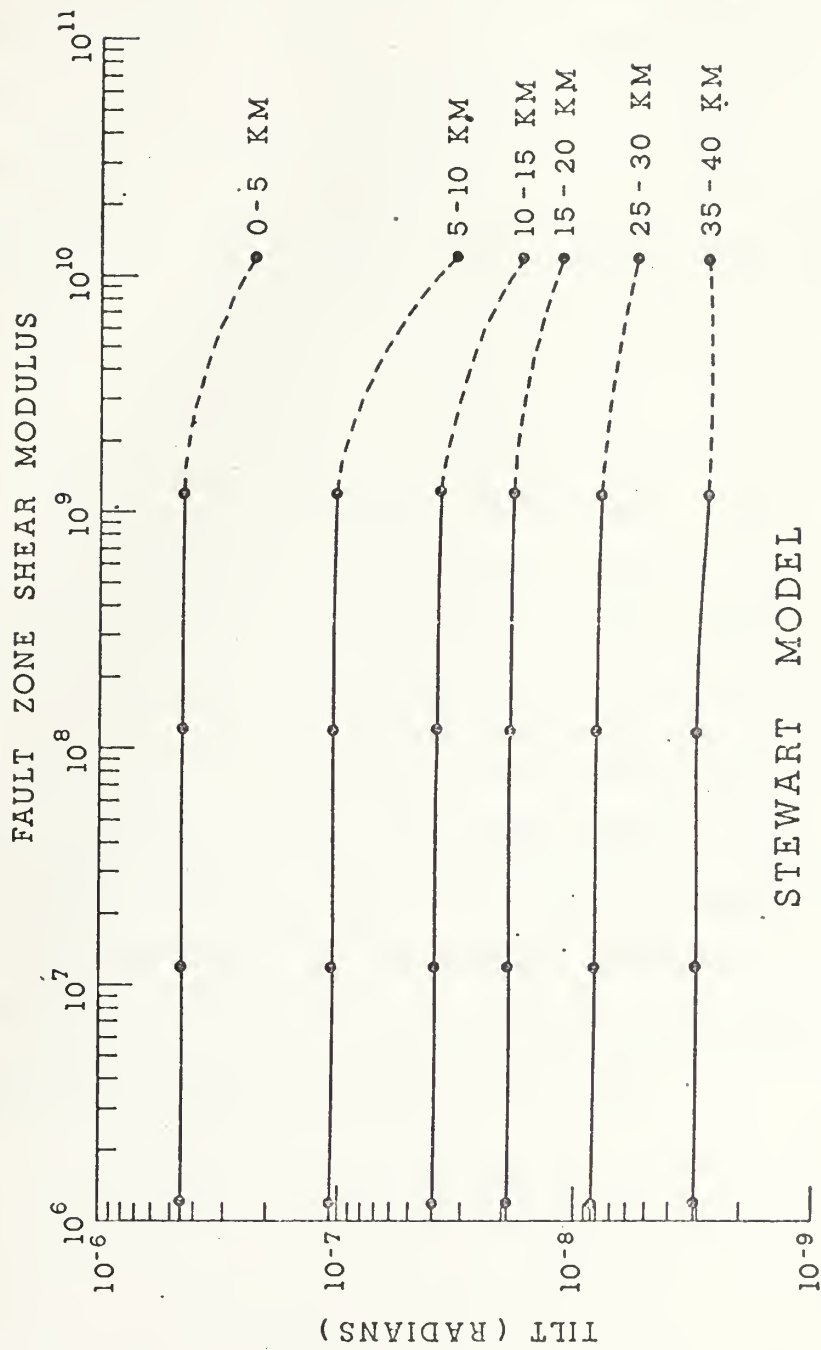


FIGURE 8

tilt and fault zone location in the range of 10 to 45 kilometers. Both the hard bottom model and the Stewart model are better models of the real Earth's velocity structure [11]. However, because of grid design constraints, the detail of the velocity structure which could be represented was limited, especially in the 0 to 15 kilometer depth range. A plot of the displacement field throughout the structure revealed a final shortcoming of the grid design. The depth used in the present model is too shallow to explore fault zone locations farther than 50 kilometers from the edge of the load. It is apparent from figure 9 that the problem of grid design is directly related to the boundary conditions of the rigid bottom edge. The rigid bottom has the tendency to make the next to bottom layer of the structure oscillate about zero centimeters displacement at distances over 50 kilometers from the load. Also, the ratio of effective distance of the load from a response point to the depth used in the model should not exceed unity. This deduction is demonstrated in figure 9 where the depth of the model structure is 61 kilometers and invalid results occurred beyond the region of 50 to 60 kilometers from the edge of the load.

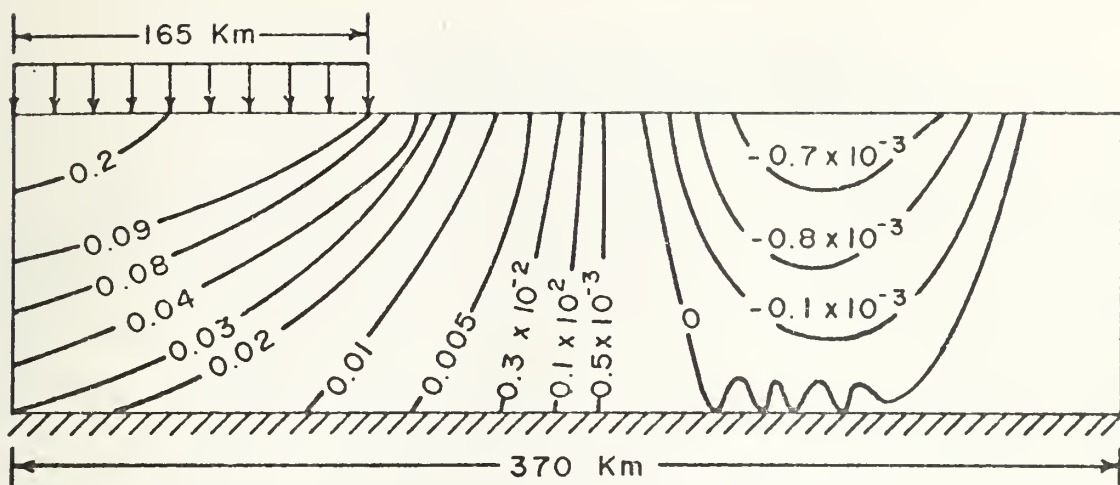


Figure of Displacement Field in the Hard Bottom Model

FIGURE 9

IV. MODELS OF FOUR PROFILES OF THE CALIFORNIA COASTLINE

Four profiles of the California coastline were modeled using the finite element technique in an attempt to compare the results with data collected by the United States Geological Survey. However, the results of these investigations point out pitfalls in the modeling phase. The four profiles are pictured in Figure 10. For reasons given below, the only useful profile is profile A. Figure 11 shows the displacement of the surface nodes plotted against distance. Figure 11 also depicts the location of the loading and the location of the fault zone. The upper dotted line results when a fault zone shear modulus is one order of magnitude less than the shear modulus of adjacent surface elements. The lower curve is based on the assumption that no fault zone exists and the elements in the fault zone are therefore identical with those adjacent to the zone at the same depth. The fault zone tilt associated with the no fault structure was 4.18×10^{-7} radians whereas the fault zone curve has a calculated tilt of 2.09×10^{-5} radians. This tilt was expected from the graphs developed in the previous chapter and is comparable to actual tilt data in the San Francisco Bay area. Figures 12, 13, 14 display the same attributes for profiles B, C, and D as that of Figure 11 of profile A. In profiles B, C, and D the ocean loading was not sufficient in magnitude to accurately model ground movement in these profiles. This resulted in the instabilities

discussed in the previous chapter. At least 165 kilometers or more of ocean loading is required to provide an adequate forcing function for the modeling of all profiles. Zones of 2.5 kilometers in width are probably too small to be realized by the existing grid design. Therefore, fault zones of 2.5 kilometers in width showed little or no change in the displacement field between no-fault and fault structures. Also, as stated in the previous chapter, the grid design is too shallow to place fault zones farther than 50 kilometers from the edge of the load and receive valid information.

FOUR CALIFORNIA PROFILES

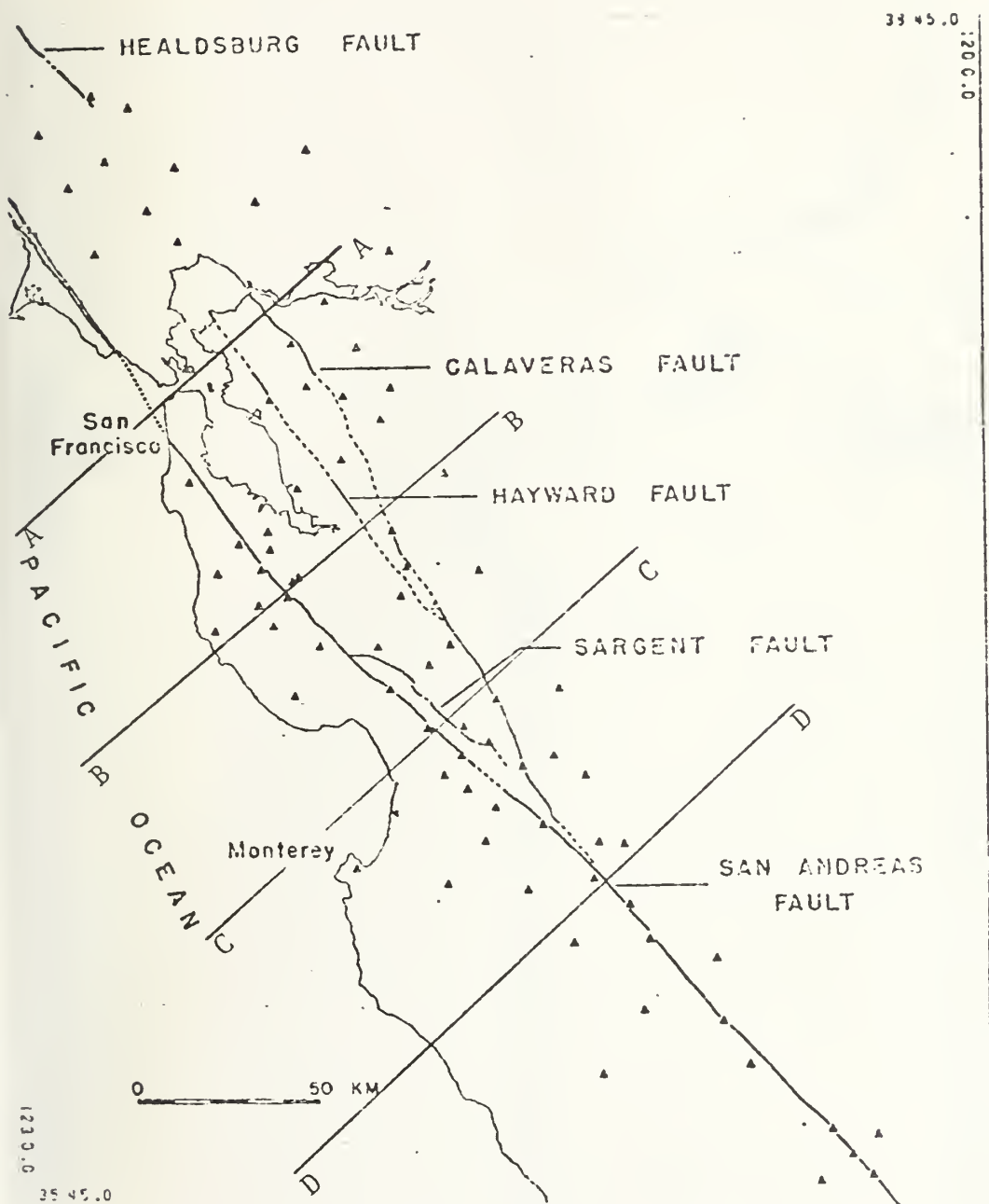


FIGURE 10

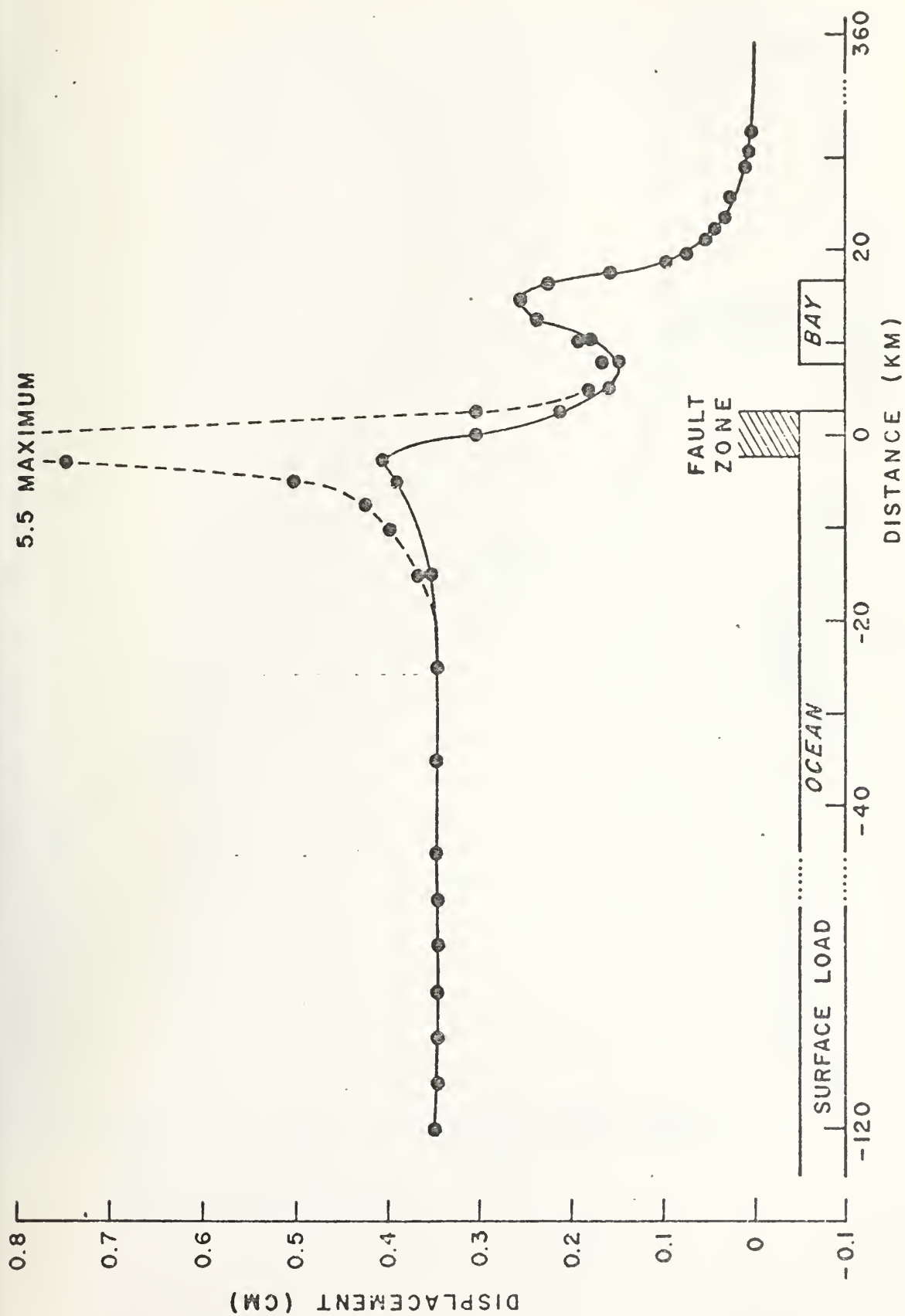


FIGURE 11

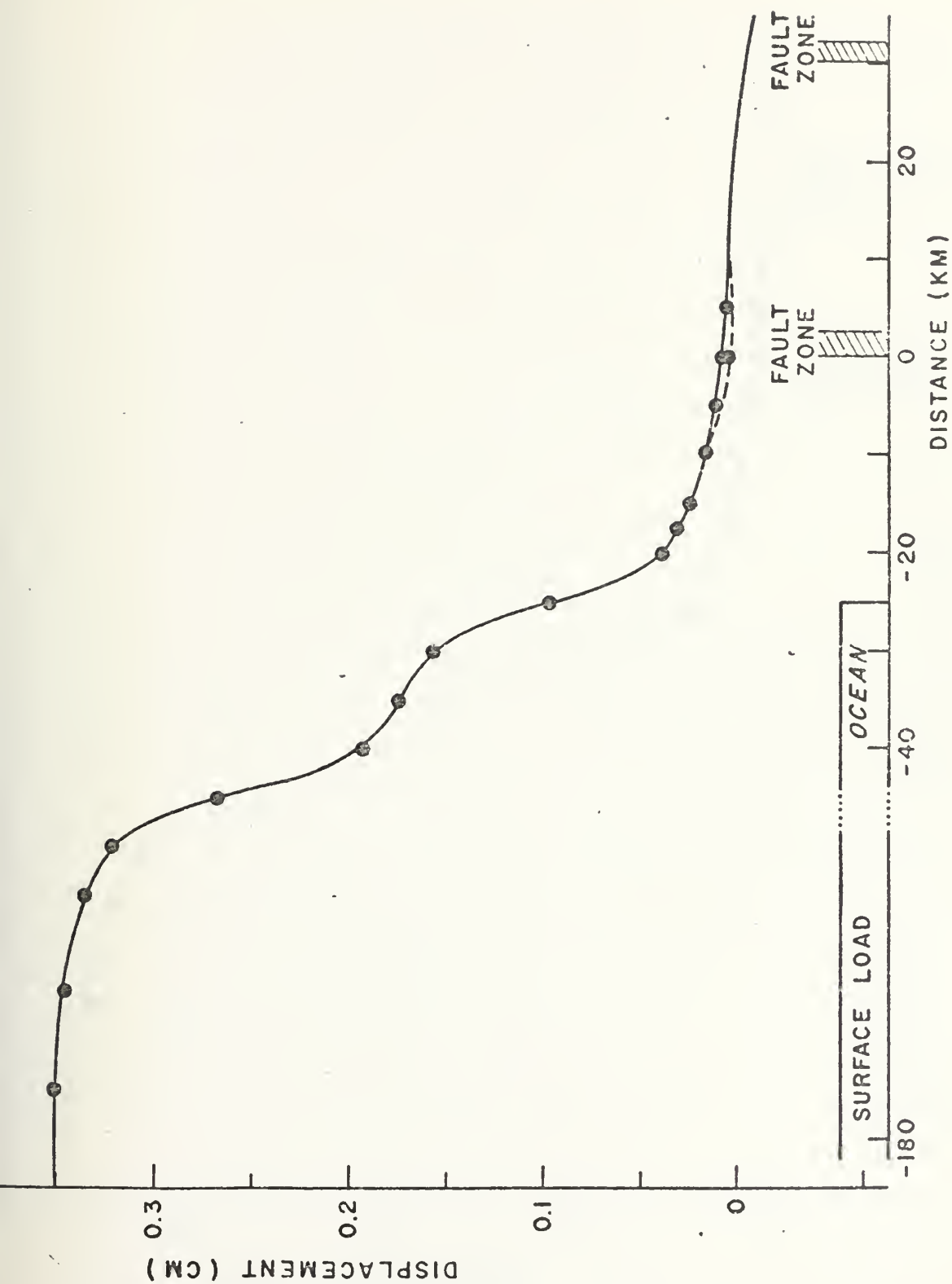


FIGURE 12

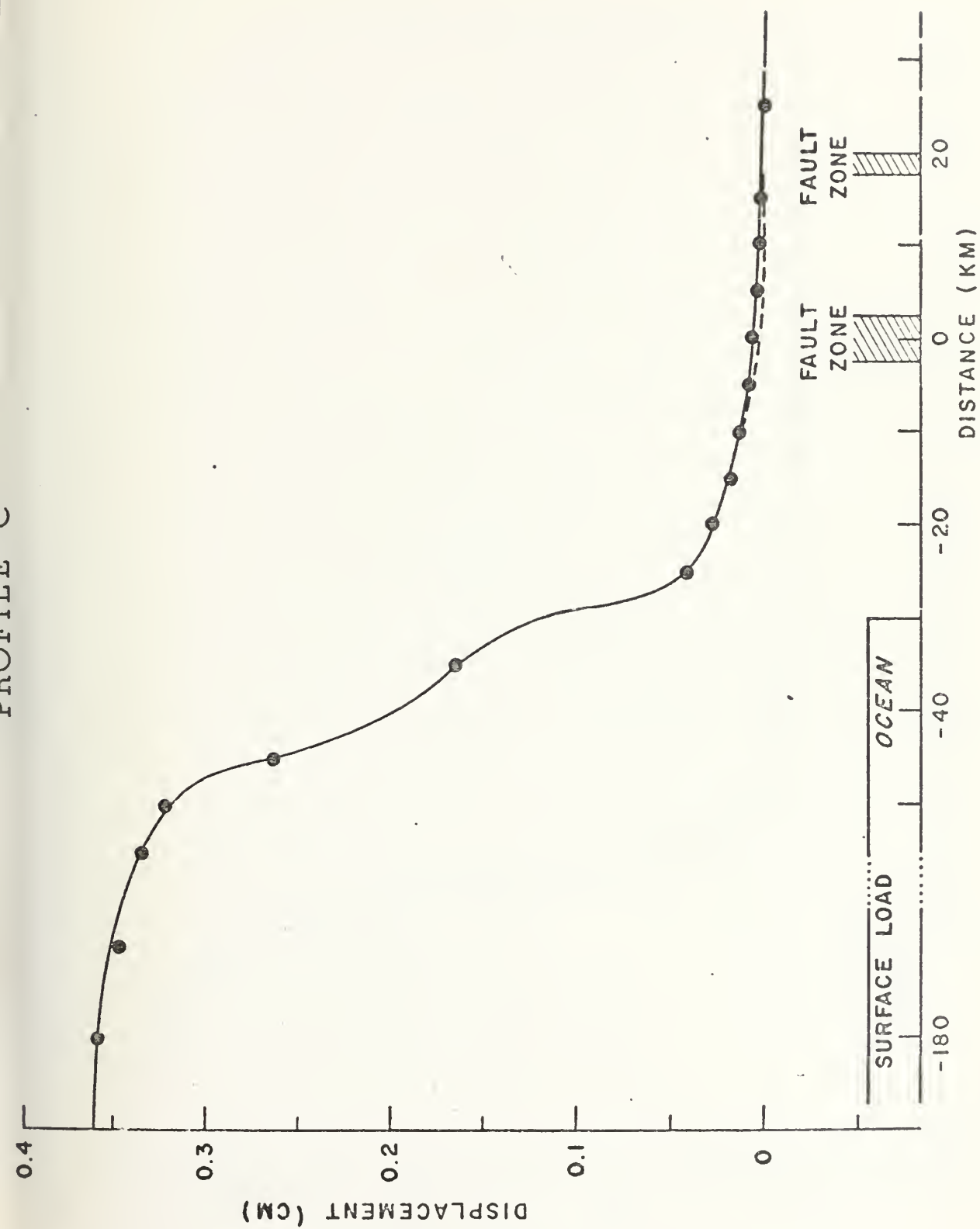


FIGURE 13

PROFILE D

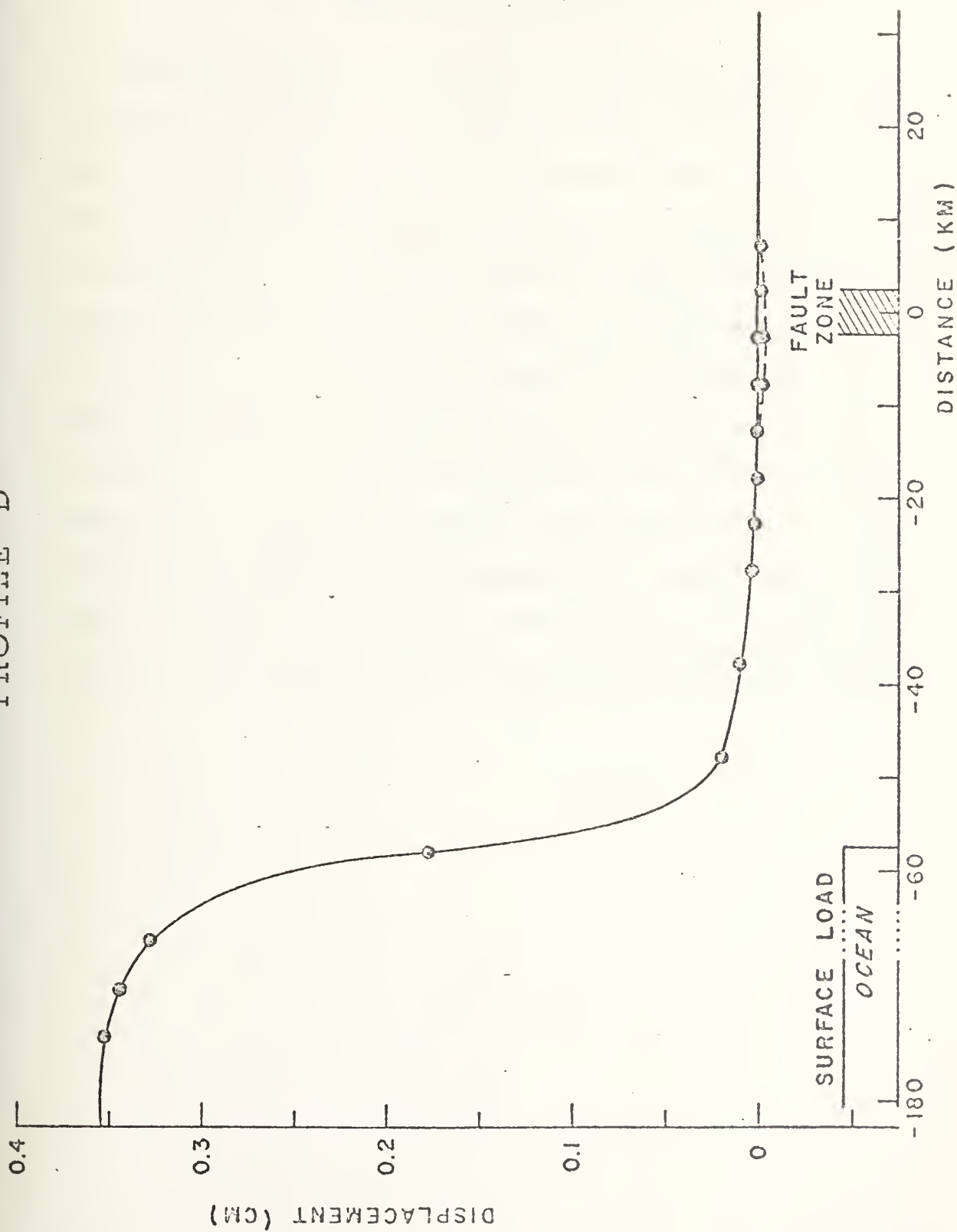


FIGURE 14

V. AREAS FOR FURTHER STUDY

Further study is definitely needed to develop the four California profiles into useable models. Modular construction of the grid is strongly encouraged when alterations are made to add further depth to the grid. Further work is needed to develop an effective and efficient three dimensional finite element computer program and model. This should provide a valuable tool for analyzing more detailed deformations resulting from a variety of loads applied to an inhomogeneous structure. This type of three dimensional finite element model could possibly be used in providing inputs to siloed missiles described in the introduction. Rainfall and barometric fluctuations could be used as the forcing functions to the finite element model instead of ocean tidal loading.

VI. CONCLUSIONS

The finite element model has demonstrated its usefulness in analyzing deformations resulting from a system of loads applied to an earth structure. If the structure is assumed to be of a homogeneous medium, then the finite element model produces results similar to that of Boussinesq models. In analyses of deformations in which the structure consists of an inhomogeneous medium the numerical method of finite elements has shown to be a most valuable asset. A logarithmic relationship between the magnitude of fault zone tilt and the distance of the fault zone from the edge of the load was shown to exist by manipulating the finite element model. Fault zone tilt was also shown to converge in magnitude for a given fault zone location when the fault zone shear modulus was decreased more than one order of magnitude from that of adjoining cells in the finite element grid.

APPENDIX A

DOCUMENTATION OF THE FINITE ELEMENT COMPUTER PROGRAM

The basic idea underlying the finite element concept is to substitute a simpler problem for the actual complex problem. If the simpler problem can be solved and if the resulting solution represents a feasible solution with acceptable accuracy, then the finite element technique has obviously served a useful purpose. The finite element method treats a continuum as an assembly of simple structural components or elements which are connected at a finite number of points, called nodes.

The process of fitting a variety of geophysical measurements to the array of possible earth structures and their responses requires a finite element technique. The finite element computer program used in this paper was developed to meet the need for a simple mesh or grid construction allowing for analysis of deformations of axisymmetric and plane strain elastic structures. The program is based on the theory of finite elements as presented by O. C. Ziekiewicz and Y. K. Cheung [15]. Typical finite element programs are so tedious and time consuming in the design of the mesh and indexing of the nodes and cells that they tend to inhibit a thorough investigation of the variety of models that satisfy the geophysical measurements. The finite element program in this paper solves the problems of inversion, non-uniqueness,

and convergence in an efficient and effective manner without becoming overly complex. The program has facilities for processing in one run, several models which the investigator requires for validating his hypotheses.

The computer program is written in Fortran. This facilitates using the program on different systems. The program is composed of a main program and two subroutines, named ASAPS and QPLOT.

The main program constructs the grid, indexes and positions nodes and cells, assigns associated elastic parameters, sets up boundary conditions, and places the vertical surface force in position. The construction of the grid is accomplished by the standardization of five modular mesh types. The mesh types are described as coarse, intermediate, fine, left and right link connectors. The five mesh types are shown in figure 15.

The grid is the hub of the modeling phase. It is constructed by assembling the five mesh types or any combination of mesh types into the desired structure. The dimensions of the grid may vary depending on the number of mesh types used. The grid may be designed so that nodal points are closer spaced by using the fine mesh type in areas where deformations are expected to vary most rapidly. To provide the appropriate transition from a coarse mesh to either an intermediate or fine mesh requires the appropriate right or left link connectors to be inserted. Figure 16 illustrates a completed grid design. The type of grid design which has been discussed

SAMPLE GRID MESH

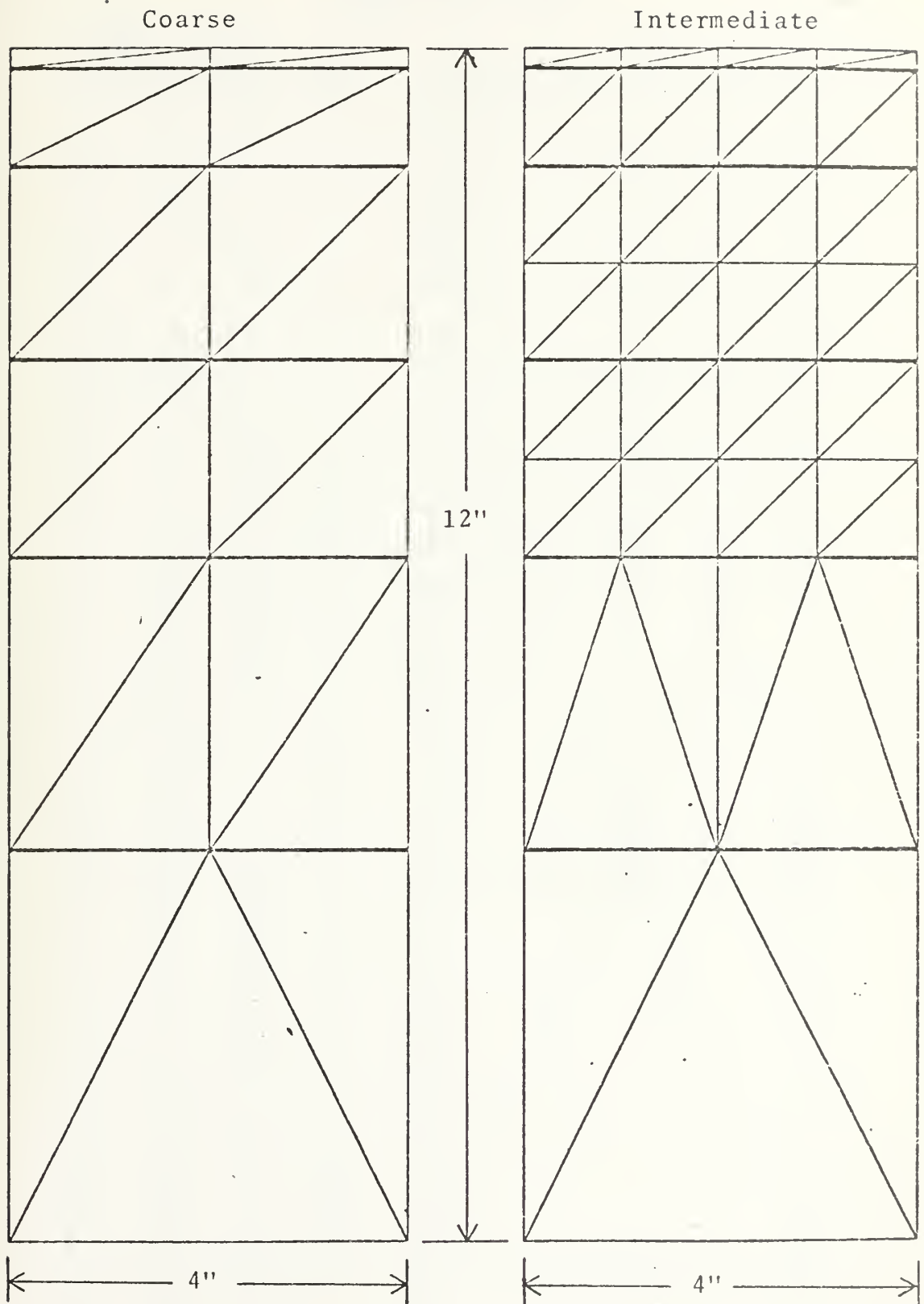


FIGURE 15A

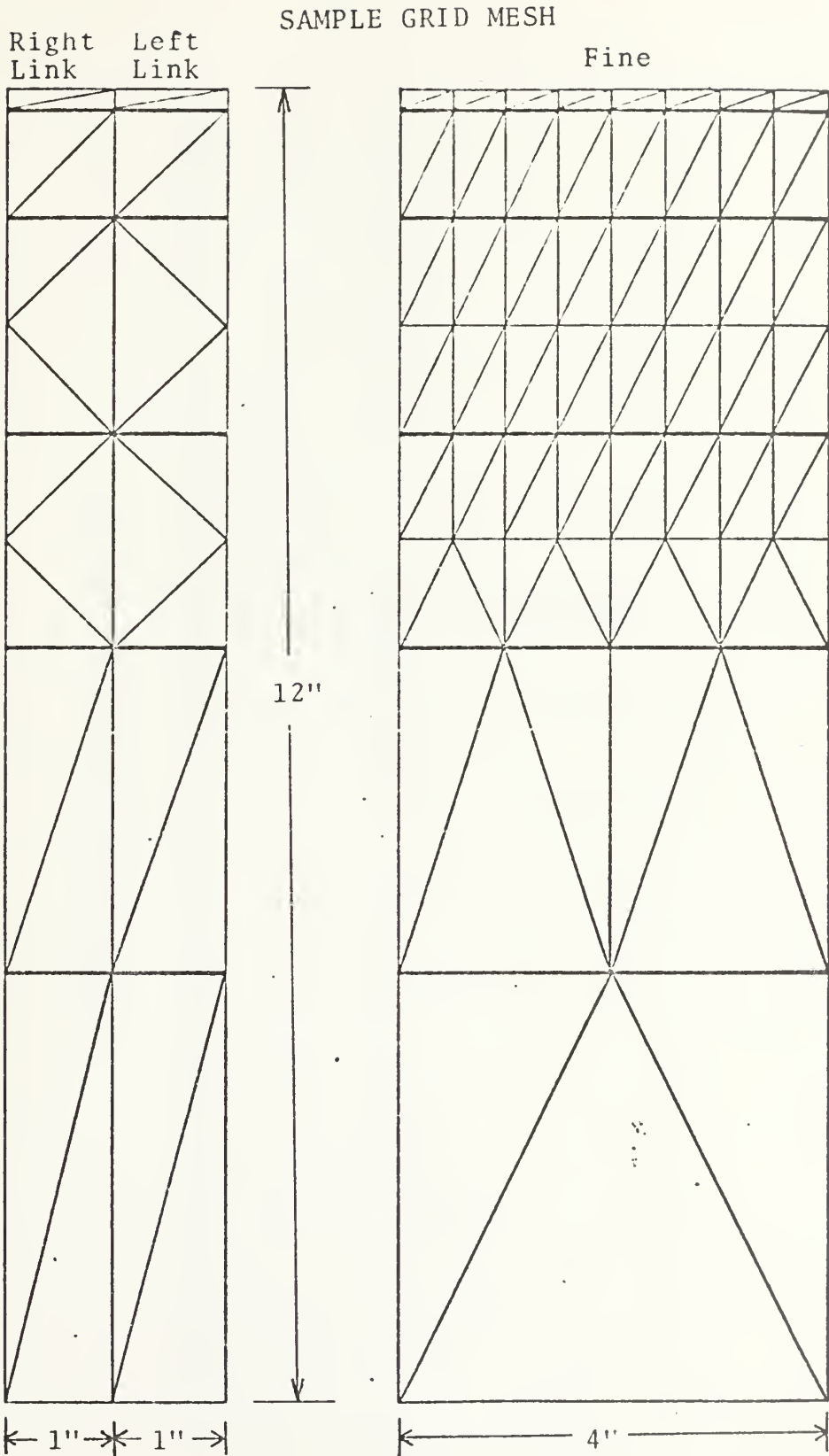
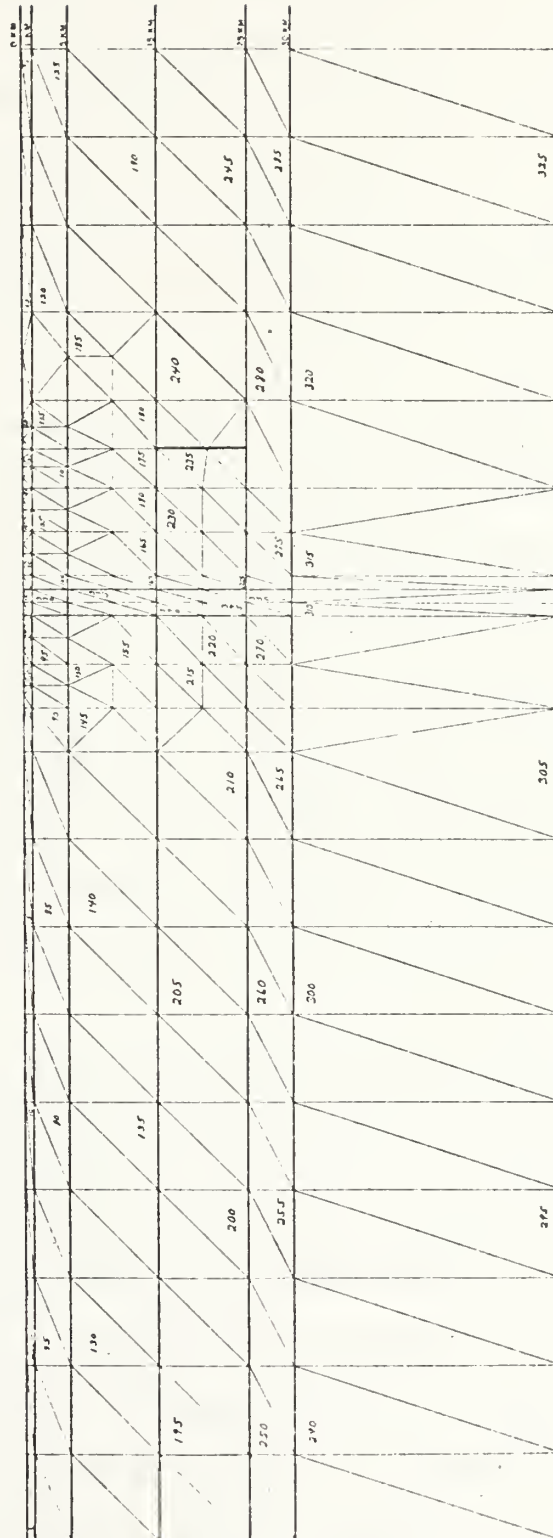


FIGURE 15B

SAMPLE OF COMPLETED GRID DESIGN



Scaling 0.2" = 1 km
 1" = 5 km
 NA = 5

FIGURE 16

above is only valid for plane strain modeling problems. Axisymmetric problems require a different type of grid which has ring-shaped elements with triangular cross sections. Thus for axisymmetric problems a manual grid construction is required and the automatic grid generator in the main program would be aborted. In any grid design the aspect ratio between the lengths of the two legs of the triangular element should not exceed 10:1.

An overlay procedure for elastic boundary conditions was devised so that structures composed of several materials are as easy to model as structures composed of a single material. Each elastic boundary condition is on a separate data card with the coordinates (in inches) which bound that particular set of elastic parameters. The overlay procedure is achieved by giving later specified boundary conditions precedence over former specified boundary conditions. This allows structures to be described by a basic structure which can be easily modified.

The ASAPS subroutine calculates the deformations of axisymmetric and plane-strain elastic structures, using the finite element technique [3]. This program employs the simple triangular element which is constrained to deform homogeneously (for axisymmetric problems the elements are ring-shaped with a triangular cross section). From the mechanical properties and dimensions of each element a stiffness matrix is formed for the entire assembly which relates nodal forces to nodal displacements. The x components and y components of nodal

displacements are the principal unknowns in the analysis and are determined from linear simultaneous equations of the form

$$F_i = \sum_{j=1}^{2N} K_{ij} D_j \quad i = 1, 2, \dots, 2N$$

where N = number of nodes

F_i = components of force at the nodes; F_i and F_{N+i} are the horizontal and vertical components of force, respectively, at the i^{th} node

K_{ij} = stiffness matrix

D_j = nodal displacement components.

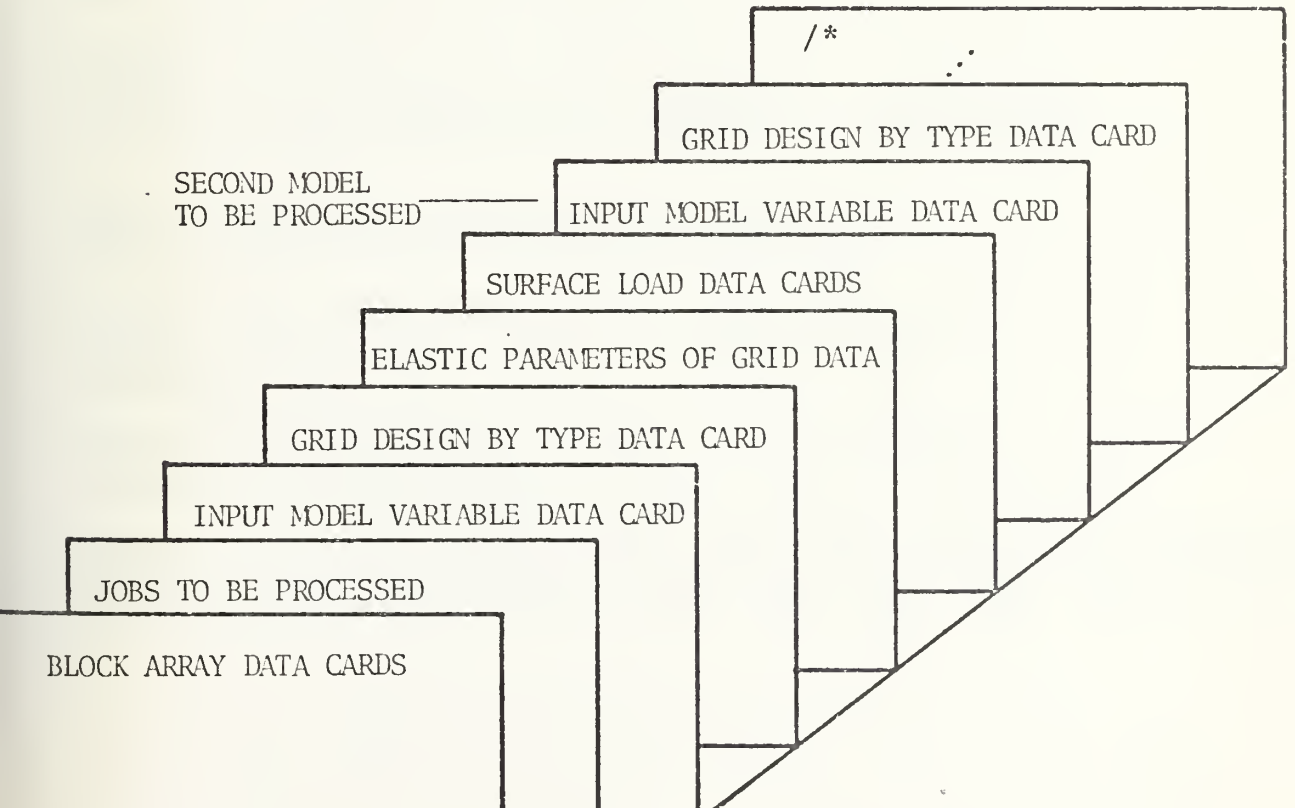
Young's overrelaxation method [5] was employed for solution of the equations. This is an iterative method used to improve the rate of convergence. The value of the overrelaxation parameter, W , must be specified with the input data. Because the optimum value of this parameter varies from problem to problem, efficient use of this method requires some experience. This inconvenience, however, is more than offset by the speed of this method and by the small amount of core which is required relative to simple and direct methods of solution. Other methods with comparable speed and storage place bothersome restrictions on the design and labeling of the finite element grid [3].

The subroutine QPLOT is a printer plot routine of the surface node displacements. It searches for the largest negative displacement and adds it to every nodal displacement. The plot then consists of all surface node displacements

plotted as a percent of the largest positive displacement. This was done to give the most clarity of detail possible to the plot. For each point on the plot, its associated surface node number and original displacements as calculated by subroutine ASAPS are printed.

Input Data Preparation

The first fifteen data cards of the data deck are called block array. They contain information about the construction of the grid from the five mesh types. These data cards are always required and always remain in the same position, regardless of the grid design. The following order of input data cards follows the block array data cards.



The above data cards in their proper formats are required to insure that the program will run successfully. The format for each parameter in the input data deck is described below.

Data Cards Supplied by Experimenter

Job Card

Columns	1 2
Format	I2
Parameter	JOB

Model Variables Data Card

Columns	1 4	5 9	10 14	15 19	20 24	25 29	30 34	35 39	40-44	45-46	47-48
Format	I4	I5	I5	I5	I5	I5	I5	F5.3	I5	I5	I5
Parameter	IPO	NBLKS	NZ	NF	KBND	IGEOM	ITERAT	W	NA	NB	NC

Grid Design by Mesh Type Data Card

Columns	1	2	3	4	NBKS
Format	I1	I1	I1	I1	I1
Parameter	NBLK(1)	NBLK(2)	NBLK(3)	NBLK(4)	NBLK(BNLKS)

Elastic Parameters of Grid Data Cards (There are NZ (Number) of These Data Cards)

Columns	1 5	6 10	11 15	16 20	21 27	28 34
Format	F5.1	F5.1	F5.1	F5.1	E7.1	E7.1
Parameter	YZ1	YZ2	YZ1	YZ2	UZ1	UZ2

Surface Loads Data Cards (There will be NF/10 (Rounded to Highest Whole Number) of these Data Cards)

Columns	1 5	6 10	11 15	16 20	21 25	26 30	31 35	36 40	41 45	46 50
Format	F5.1	F5.1	F5.1	F5.1	F5.1	F5.1	F5.1	F5.1	F5.1	F5.1
Parameter	FY	FY	FY	FY	FY	FY	FY	FY	FY	FY

The input parameters are described as follows:

JOB specifies the total number of models to be processed in one run.

IPO print option of which there are eight. The printout is divided into four parts:

- A cell numbers, locations of associated nodes and elastic parameters.
- B node numbers and location and associated values of NDISP, DISP.
- C node number and location and associated displacement.
- D diagram of vertical displacements of surface nodes.

IPO = 1 prints A, B, C, D

IPO = 2 prints B, C, D

IPO = 3 prints A, only surface nodes B, C, D

IPO = 4 prints only surface nodes B, C, D

IPO = 5 prints only data associated with surface nodes in B and C, D

IPO = 6 prints C, D

IPO = 7 prints only data associated with surface nodes in C, D

IPO = 8 prints D.

NBLKS total number of mesh types used in grid design

NZ total number of elastic boundary conditions incorporated in grid design.

NF total number of surface nodes in grid design.

KBND code for boundary conditions of the grid:

- 0 all sides free
- 1 bottom rigid
- 2 sides rigid
- 3 bottom and sides rigid.

IGEOM code for plain strain or axisymmetric type of problem:

- 1 plain strain problem and stress strain calculations in ASAPS will be bypassed.
- 2 axisymmetric problem and stress strain calculations will be accomplished in ASAPS

ITERAT number of iterations taken for solution of simultaneous equations.

W overrelaxation parameter used to reduce solution time and speed convergence. Value should be between 1.6 and 1.7.

NA exponent of ten used as scale factor for nodal coordinates.

NB exponent of ten used as scale factor for surface nodal forces.

NC exponent of ten used as scale factor for nodal displacement (zero if cm. is required and cgs units are used for NA and NB)

ND exponent of ten used as scale factor for elastic parameters (Lame's constants). If elastic parameters are loaded in exponential form, then ND = 0.

NBLK subscripted variable containing coded quantity: of the grid design by mesh type.

- 1 course
- 2 left link connector
- 3 intermediate
- 4 fine
- 5 right link connector

YZ1 Y coordinate of top left hand corner of boundary condition (in grid coordinates, i.e., inches)

YZ2 Y coordinate of bottom left hand corner of boundary condition (in grid coordinates, i.e., inches)

XZ1 X coordinate of top right hand corner of boundary condition (usually zero and also in grid coordinates, i.e., inches)

XZ2 X coordinate of bottom right hand corner of boundary condition (in grid coordinates, i.e., inches).

UZ1 Lamé constant Lamda (λ) coefficient of elasticity.

UZ2 Lamé constant Mu (μ) coefficient of elasticity.

FY(I) normal force at each of the surface nodes.

Example calculation for solving Lamé's constants given a velocity structure:

Find λ and μ for the sample velocity structure in the zone where $v_p = 6.0$ km/sec assuming Poisson ratio of .25.

$$\text{Poisson ratio } \sigma = \frac{\lambda}{2(\lambda + \mu)} \quad (1)$$

$$\text{Velocity for elastic waves (longitudinal waves, P waves)} v_p = \left(\frac{\lambda + 2\mu}{\rho} \right)^{1/2} \quad (2)$$

where ρ = density and is obtained from the Nafe-Drake curve which displays the variation of density with P wave velocity.

$$\text{For } v_p = 6.0 \text{ km/sec} \implies \rho = 2.75 \text{ g/cm}^3$$

Now, solving equations 1 and 2 above simultaneously for λ and μ .

Equation 1

$$.25 = \frac{\lambda}{2(\lambda + \mu)}$$

$$.5 = \frac{\lambda}{\lambda + \mu}$$

$$.5\lambda + .5\mu = \lambda$$

$$\lambda = \lambda$$

Equation 2

$$6 \times 10^5 = \left(\frac{\lambda + 2\mu}{2.75} \right)^{1/2}$$

$$6 \times 10^5 = \left(\frac{3\lambda}{2.75} \right)^{1/2}$$

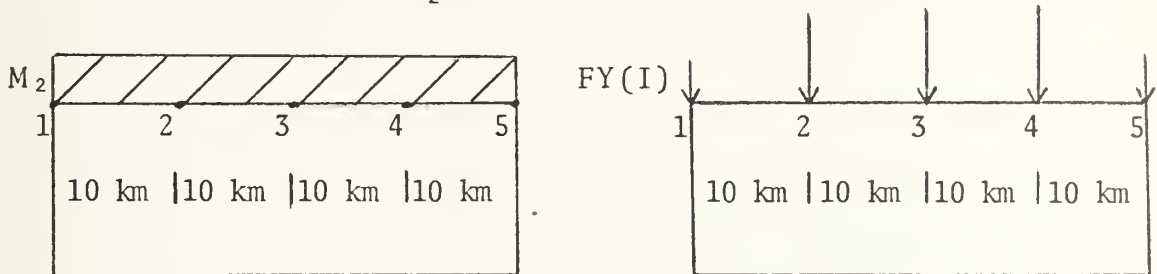
$$\lambda = 3.3 \times 10^{11}$$

$$\mu = 3.3 \times 10^{11} \text{ dynes/cm}^2$$

ANS.

Example calculation for determining scale factor (NB) and normal surface forces (FY) given the amplitude of the M_2 frequency of third tidal spectrum.

Find $FY(I)$, given $M_2 = 50$ centimeters?



$$\text{Force} = \text{Pressure} \cdot \text{Area}$$

$$\begin{aligned} \text{Pressure} &= \rho g h = 1 \text{ g/cm}^3 \times 9.8 \times 10^2 \text{ cm/sec}^2 \times 50 \text{ cm} \\ &= 4.9 \times 10^4 \end{aligned}$$

where ρ = density of sea water

g = gravity

h = amplitude of M_2

$$\begin{aligned} \text{Area} &= \text{Distance between nodes} \cdot 1 \text{ cm} \\ &= 10 \times 10^5 \text{ cm}^2 \end{aligned}$$

(Note: 1 cm is assumption of unit width of surface load.)

$$\text{Force} = 4.9 \times 10^4 \times 10 \times 10^5 = 49 \times 10^9 \text{ dynes at each interior node.}$$

$$NB = 9.$$

Nodes located at edges of load should be loaded with half as much force, to simulate a uniform load.

Derivation of NA for coordinate system in kilometers:

Let smallest mesh distance (.2 inches) equal 1 km.

$$\text{Then } .2 \text{ inches} = 1 \text{ km} = 1 \times 10^5 \text{ cm}$$

$$.5 \text{ inches} = 2.5 \text{ km} = 2.5 \times 10^5 \text{ cm.}$$

$$1 \text{ inch} = 5 \text{ km} = 5 \times 10^5 \text{ cm}$$

therefore $NA = 5$.

Core Requirements

Core requirements obviously depend upon the size of the grid (i.e., the total number of cells and nodes). Variables O, P, Q, XC, YC, AREN, ELAM, and EMU are subscripted in common with the total number of cells in the grid. Variables XF, YF, FX, FY, MID, LID, and LIDS are subscripted in common with the total number of nodes in the grid. Finally, variables A, AR, B, MAP, NDISP, and DISP are subscripted in common with twice the total number of nodes in the grid. A program with 744 cells and 419 nodes required 280 K bits of core on an IBM 360-67 computer. This was a very large grid spanning 74 modeling inches. For most grids of 500 cells or less, 200 K bits of core would be sufficient to run the program, on an IBM 360-67 computer. Of course, core requirements will differ from system to system. The above mentioned core requirements are meant to be a guide.

Time Requirements

The time required to run the finite element computer program is a function of the grid size, the number of iterations required to obtain a convergent solution and the amount of printout required. An IBM 360-67 computer required approximately fifteen minutes to process a 744 cell, 74 inch model grid using 1,000 iterations and a complete printout (IPO = 1). This time may be considerably reduced if only information about the surface displacements is required. Using IPO = 8 on the same grid and 1,000 iterations only eight minutes was

required to run the program. Again, if IPO = 8 is used on the same grid and only 300 iterations are required the program ran in four minutes. Of course, time requirements will differ depending on the system and the overhead required. The above mentioned time requirements are meant as a guide.

Internal Forces

Internal forces can be processed by this finite element computer program in conjunction with surface loads or instead of surface loads. However, each internal node force must be loaded manually into the program by inserting the appropriate instruction in the main program. The calculation of the size of the nodal force is the same as if it were a surface force. The sign of the force specified determines force direction. Positive force is a downward force and a negative force is an upward force. The internal force at node I should be loaded in the following format,

$FY(I) = (\pm)(\text{force size}) * 10.** \text{ NB}$

The internal force statements should be inserted between statement numbers FETO3590 and FETO3600 in the main program. If only internal forces are desired, blank data cards should be used in the input section for surface loads in the data deck.

Cutout Procedure

A problem faced by the experimenter is determination of a number of iterations sufficient to be assured that the solution has converged. This must be specified in the input data ITERAT. A number which far exceeds the point of

convergence wastes computer time and money. Therefore, in subroutine ASAPS variable CUT is specified in statement number FETO4700. It is now arbitrarily set at 0.000001. CUT is compared with the percentage difference that some surface node has displaced in 25 iterations. Thus CUT is a percentage beyond which the experimenter feels the solution has converged and wishes to terminate the procedure. The surface node used for the comparison should be located either under the load system or in a zone where a large amount of deformation is expected to take place. The node number is determined by variable MIS specified in statement number FETO4680 in the ASAPS subroutine. However, if the experimenter knows how many iterations are required and specifies that number in the input data, he may desire to by-pass the cutout procedure. This is accomplished by changing statement number FETO6860 in ASAPS

```
from 901 IF(PERC.LE.CUT) GO TO 902  
to    901 IF(PERC.LE.CUT) GO TO 104.
```


Definitions of Non-Input Variables

DISP(I) displacement in x-direction of node I (cgs units)

DISP(I+NODE) displacement in y-direction of node I

FX(I) horizontal force at node I

NCELL total number of cells in grid

NDISP(I) = 1 displacement is set at 0.1, i.e., node I
is rigid in x-direction
= 0 displacement is unspecified at node I in
x-direction

NDISP(I+NODE) same as NDISP(I) except in y-direction

NODE total number of nodal points in grid

O(I) node number of uppermost left node in cell I

P(I) clockwise node number from O(I) in cell I

Q(I) clockwise node number from P(I) in cell I

XF(I) x coordinate of node I

YF(I) y coordinate of node I

AREN(I) area of cell I

IBL(I) the node number beginning layer I of the grid
(fine and intermediate have 9 layers
course has 7 layers)

IEL(I) the node number that ends layer I of the grid

CUT percentage change in the distance that some surface
node (determined by MIS) moves in 25 iterations.
(See cutout procedure)

LISTING OF FINITE ELEMENT TECHNIQUE COMPUTER PROGRAM

```

COMMON O(750),P(750),Q(750),XC(750,3),YC(750,3),ZC(750,3),
2XF(425),YF(425),FX(425),FY(425),NDISP(0850),DISP(0850),
3 XZ1(025),XZ2(025),YZ1(025),YZ2(025),UZ1(025),UZ2(025),
4A(850,16),AREN(750),AR(850),B(850),ELAM(750),EMU(750),
5LIDS(425,7),LID(425,8,2),MAP(850,16),MID(425,8),
6NA,NB,NC,ND,NODE,NCELL,IGEOM,ITERAT,W,NF,IPO
INTEGER O,P,Q,ON,PQ,ON,QN,QTEMP,CE,PE,QE
DIMENSION NBLK(50),BLK(5,3,10),LAY(10),IEL(10),IBL(10)

XF,YF,FX,FY,MID,LID,LIDS.....N TOTAL NUMBER NODES
O,P,Q,XC,YC,AREN,ELAM,EMU.....M TOTAL NUMBER CELS
A,AR,B,MAP,NDISP,DISP.....2N

CODE TYPE CELLS NODES L,R LNK
1 COARSE 23 20 7,7
2 L.LNK 14 16 7,7
3 INT 57 40 9,9
4 FINE 101 64 9,9
5 R.LNK 14 16 9,7

FORMAT(1X,'END DUE TO VARIABLE NBLKS EQUAL ZERO')
FORMAT(1X,'END DUE TO VARIABLE NZ EQUAL ZERO')
FORMAT(1X,'END DUE TO VARIABLE NF EQUAL ZERO')
FORMAT(2I5,6F5.1)
FORMAT(8F10.2)
FORMAT(2I5)
FORMAT(14,6I5,F5.3,4I5)
FORMAT(10F5.1)
FORMAT(50I1)
FORMAT(10X,7F10.2,2I5)
FORMAT(4F5.1,2E7.1)
FORMAT(15,4F10.2,2E10.2,15)
FORMAT(12)
FORMAT(10F5.1)
FORMAT(15,3E12.4,3(E12.4,I5))
FORMAT(1H1,50X,'BLK MATRIX (5,3,10) REMAINS CONSTANT',//)
FORMAT(10X,'DATA CARD',/,20X,'IPO NBLKS NZ NF KBND IGEOM ITERA
1T W NA NB NC ND',/)
FORMAT(19X,14,5I5,3X,I5,3X,F5.3,4I5,/)
FORMAT(1X,'AREA',6X,'XZ1',7X,'XZ2',7X,'YZ1',7X,'YZ2',7X,'UZ1',7X,
1,UZ2',2X,'ARLA',/)
FORMAT(1H1,3X,4HCELL,1X,'O X-COORD',3X,'O Y-COORD',3X,
1,P X-COORD',3X,'P Y-COORD',3X,'Q X-COORD',3X,'Q Y-COORD',4X,1H0,4X
2,1HP,4X,1HQ,6X,5HLAMDA,6X,2HMU,4X,4HCELL)
FORMAT(1H1,1X,4HNODE,3X,7HX-COORD,5X,7HY-COORD,3X,6HXFORCE,9X,

```



```

16HYFORCE,4X,6HNDISPX,1X,5HDISPY,1X,6HNDISPY,4X,5HDISPY,4X,4HNDDE,
23X,NOTE COORD IN CGS UNITS',//)
903 FORMAT(15,6E12.4,3I5,2E12.4,15)
904 FORMAT(15,8F10.2)
905 FORMAT(4I5,6F10.2)
9033 FORMAT(1X,15,6E12.4,3I5,2X,2E10.2,2X,13)
9034 FORMAT(10X,/,NOTE COORD IN MESH UNITS',//)
C WRITE(6,720)
DO 59 I=1,5
DO 59 J=1,3
C READ(5,104) (BLK(I,J,K),K=1,10)
C WRITE(6,104) (BLK(I,J,K),K=1,10)
59 CONTINUE
C
C INPUT CARD*****JOB=NUMBER OF MODELS TO BE PRECESSED
C THIS CARD PRECEDES DATA FOR MODELS (FORMAT12)
C
C READ(5,666) JOB
C DO 1000 NNK=1,JOB,1
C
C INPUT CARD
C IPO=OUTPUT PRINT OPTION PRINT OUT IS IN FOUR PARTS
C A-CELLNUMBERS, LOCATION OF ASSOCIATED NODES, LAMDA, MU
C B-NODES AND THEIR ASSOCIATED LOCATION, NOISP, DISP
C C-DISPLACEMENTS IN X AND Y DIRECTION OF NODES
C D-PRINTER PLOT OF SURFACE NODES
C IPO=1 PRINTS A,B,C,D
C IPO=2 PRINTS B,C,D
C IPO=3 PRINTS A, ONLY SURFACE NODES IN B,C,D
C IPO=4 PRINTS A, ONLY SURFACE NODES IN B,C,D
C IPO=5 PRINTS C, ONLY DATA ASSOCIATED WITH SURFACE NODES IN B AND C,D
C IPO=6 PRINTS C,D
C IPO=7 PRINTS ONLY DISPLACEMENTS OF SURFACE NODE C,D
C IPO=8 PRINTS ONLY D
C NBLKS=TOTAL NUMBER OF MESH TYPES USED IN GRID CONSTRUCTION
C NZ=NUMBER ELASTIC BOUNDARY FIELDS.
C NF=NUMBER SURFACE NODES.
C KRND=0 ALL SIDES FREE (1) BOTTOM FIXED (2) SIDES FIXED (3) BOTTOM
C AND SIDES FIXED
C ICEOM=1 IF STRESS-STRAIN CALCULATIONS IN SUBROUTINE ASAPS ARE TO
C BE BYPASSED. OTHERWISE ICEOM CAN BE ANY OTHER INTEGER.
C ITERAT=NUMBER ITERATIONS TAKEN FOR SOLUTION OF SIMULTANEOUS
C EQUATIONS IN SUBROUTINE ASAPS.
C NA,NB,NC,ND=EXONENT OF TEN USED AS SCALE FACTORS
C NA--X, Y, Z, XF, YF (DIMENSIONS OF MESH, COORDINATES OF NODES)
C NB--FY (NORMAL FORCE)
C NC SCALE FACTOR FOR DISPLACEMENTS
C ND--ELAM, EMU (ELASTIC PARAMETERS)
C W OVERRELAXATION PARAMETER 1.6<W<1.7

```



```

C      WRITE(6,721)      IPO,NBLKS,NZ,NF,K6ND,IGEOM,ITERAT,W,NA,NB,NC,ND
C      READ(5,103)      IPO,NBLKS,NZ,NF,K6ND,IGEOM,ITERAT,W,NA,NB,NC,ND
C      WRITE(6,722)      IPO,NBLKS,NZ,NF,K6ND,IGEOM,ITERAT,W,NA,NB,NC,ND
C      IF (NBLKS.EQ.0) GO TO 1111
C
C      INPUT CARD
C      NBLK(1)=TYPE OF I(TH) SECTION OF MESH, READING FROM LEFT TO RIGHT.
C      IE., SEQUENCE OF COARSE, L.LNK,INT., FINE, R.LNK IS READ IN AS 123
C
C      READ(5,105) (NBLK (I),I=1,NBLKS)
C      X=0.
C      Y=0.
C      K=0
C      IBLK1=NBLK(1)
C      XMX=0
C      YMX=12.
C      DU 50 KN=1,NBLKS
C      I=NBLK (KN)
C      Y=0
C      X=XMX
C      XX=BLK(I,1,10)
C      XMX=XMX+XX
C      IF(KN.EQ.1) X=0
C      DO 51 J=1,9
C      IC=BLK(I,3,J)
C      IF(IC.EQ.0) GO TO 50
C      XV=BLK(I,1,J)
C      YV=BLK(I,2,J)
C      WRITE (6,905) KN,J,K,IC,X,Y,XV,YV,XMX,XX
C      GO TO (501,502,503,504),IC
C      1009 CONTINUE
C      XVV=XV
C      IF (IC.EQ.2.OR.IC.EQ.5) XVV=2.*XV
C      IF(X+XVV-XMX) 511,513,513
C      X=X+XVV
C      511 GO TO (501,502,503,504),IC
C      Y=Y+YV
C      513 IF(Y-YMX) 52,50,50
C      X=XMX-XX
C      52 GO TO 51
C      K=K+1
C      501 XC(K,1)=X
C      YC(K,1)=Y
C      XC(K,2)=X+XV
C      YC(K,2)=Y
C      XC(K,3)=X
C      YC(K,3)=Y+YV
C      K=K+1
C      XC(K,1)=X+XV
C      YC(K,1)=Y

```

```

FET00960
FET00970
FET00980
FET00990
FET01000
FET01010
FET01020
FET01030
FET01040
FET01050
FET01060
FET01070
FET01080
FET01090
FET01100
FET01110
FET01120
FET01130
FET01140
FET01150
FET01160
FET01170
FET01180
FET01190
FET01200
FET01210
FET01220
FET01230
FET01240
FET01250
FET01260
FET01270
FET01280
FET01290
FET01300
FET01310
FET01320
FET01330
FET01340
FET01350
FET01360
FET01370
FET01380
FET01390
FET01400
FET01410
FET01420
FET01430
FET01440
FET01450

```



```

XC(K,2)=X+XV
YC(K,2)=Y+YV
XC(K,3)=X
YC(K,3)=Y+YV
GO TO 1009
CONTINUE

```

502

```

K=K+1
XC(K,1)=X
YC(K,1)=Y
XC(K,2)=X+XV
YC(K,2)=Y
XC(K,3)=X
YC(K,3)=Y+YV
K=K+1
XC(K,1)=X+XV
YC(K,1)=Y
XC(K,2)=X+2*XV
YC(K,2)=Y+YV
XC(K,3)=X
YC(K,3)=Y+YV
K=K+1
XC(K,1)=X+XV
YC(K,1)=Y
XC(K,2)=X+2*XV
YC(K,2)=Y
XC(K,3)=X+2*XV
YC(K,3)=Y+YV
GO TO 1009
CONTINUE

```

503

```

K=K+1
XC(K,1)=X
YC(K,1)=Y
XC(K,2)=X+XV
YC(K,2)=Y
XC(K,3)=X+XV
YC(K,3)=Y+YV/2.
K=K+1
XC(K,1)=X
YC(K,1)=Y
XC(K,2)=X+XV
YC(K,2)=Y+YV/2
XC(K,3)=X
YC(K,3)=Y+YV
K=K+1
XC(K,1)=X+XV
YC(K,1)=Y+YV/2.
XC(K,2)=X+XV
YC(K,2)=Y+YV
XC(K,3)=X
YC(K,3)=Y+YV

```

```

FET01460
FET01470
FET01480
FET01490
FET01500
FET01510
FET01520
FET01530
FET01540
FET01550
FET01560
FET01570
FET01580
FET01590
FET01600
FET01610
FET01620
FET01630
FET01640
FET01650
FET01660
FET01670
FET01680
FET01690
FET01700
FET01710
FET01720
FET01730
FET01740
FET01750
FET01760
FET01770
FET01780
FET01790
FET01800
FET01810
FET01820
FET01830
FET01840
FET01850
FET01860
FET01870
FET01880
FET01890
FET01900
FET01910
FET01920
FET01930
FET01940
FET01950

```


FET01960
 FET01970
 FET01980
 FET01990
 FET02000
 FET02010
 FET02020
 FET02030
 FET02040
 FET02050
 FET02060
 FET02070
 FET02080
 FET02090
 FET02100
 FET02110
 FET02120
 FET02130
 FET02140
 FET02150
 FET02160
 FET02170
 FET02180
 FET02190
 FET02200
 FET02210
 FET02220
 FET02230
 FET02240
 FET02250
 FET02260
 FET02270
 FET02280
 FET02290
 FET02300
 FET02310
 FET02320
 FET02330
 FET02340
 FET02350
 FET02360
 FET02370
 FET02380
 FET02390
 FET02400
 FET02410
 FET02420
 FET02430
 FET02440
 FET02450

```

504 GO TO 1009
    CONTINUE
    K=K+1
    XC(K,1)=X
    YC(K,1)=Y
    XC(K,2)=X+XV
    YC(K,2)=Y
    XC(K,3)=X
    YC(K,3)=Y+YV/2.
    K=K+1
    XC(K,1)=X+XV
    YC(K,1)=Y
    XC(K,2)=X+XV
    YC(K,2)=Y+YV
    XC(K,3)=X
    YC(K,3)=Y+YV/2.
    K=K+1
    XC(K,1)=X
    YC(K,1)=Y+YV/2.
    XC(K,2)=X+XV
    YC(K,2)=Y+YV
    XC(K,3)=X
    YC(K,3)=Y+YV
    GO TO 1009
51 CONTINUE
50 CONTINUE

C C C
    FIND AND REPLACE (REDUCE) ALL COMMON NODES TO LOWEST ORDER

J1=0
K7=0
DY=0.2
DX=0.5
K6=0
X=0
Y=0
YMX=12.2
XMX=0
DO 969 N=1,NBLKS
  KN=ABLK(N)
  XMX=XMX+BLK(KN,1,10)
  XMX=(5.*XMX)*10.**NA
  YMX=(5.*YMX)*10.**NA
  NYI=2+YMX
  NXI=1+XMX/DX
DO 950 I=1,NYI
DO 951 I=1,NXI
K7=0
IH=0
DO 953 I=1,K
  
```



```

DO 955 L=1,3
IF(XC(I,L).GE.X.AND.XC(I,L).LT.X+DX.AND.
C YC(I,L).GE.Y.AND.YC(I,L).LT.Y+DY)GO TO 952
GO TO 955
952 K7=K7+1
IF(IH.EQ.0)J1=J1+1
J1=J1
IH=I
GO TO (1,2,3),L
1 O(I)=JT
GO TO 954
2 P(I)=JT
GO TO 954
3 Q(I)=JT
954 CONTINUE
955 GO TO 953
953 CONTINUE
951 X=X+DX
CONTINUE
X=0
Y=Y+DY
DY=1
950 CONTINUE
959 CONTINUE
DO 909 J=1,K
WRITE(6,903) J,XC(J,1),YC(J,1),XC(J,2),YC(J,2),XC(J,3),YC(J,3),
C 20(J),P(J),Q(J)
909 CONTINUE
NCELL=K
IF(O(K).GE.P(K).AND.O(K).GE.Q(K)) NODE=O(K)
IF(P(K).GE.O(K).AND.P(K).GE.Q(K)) NODE=P(K)
IF(Q(K).GE.O(K).AND.Q(K).GE.P(K)) NODE=Q(K)
DO 703 J=1,K
I=O(J)
XF(I)=(5.*XC(J,1))*10.**NA
YF(I)=(5.*YC(J,1))*10.**NA
I=P(J)
XF(I)=(5.*XC(J,2))*10.**NA
YF(I)=(5.*YC(J,2))*10.**NA
I=Q(J)
XF(I)=(5.*XC(J,3))*10.**NA
YF(I)=(5.*YC(J,3))*10.**NA
CONTINUE
703 IF(NZ.EQ.0) GO TO 1112
WRITE(6,723)
DO 20 N=1,NZ
C INPUT CARDS
C ELASTIC BOUNDARY FIELDS MAY OVERLAP I.E. ARE INDEPENDENT OF MESH

```

FET02460
FET02470
FET02480
FET02490
FET02500
FET02510
FET02520
FET02530
FET02540
FET02550
FET02560
FET02570
FET02580
FET02590
FET02600
FET02610
FET02620
FET02630
FET02640
FET02650
FET02660
FET02670
FET02680
FET02690
FET02700
FET02710
FET02720
FET02730
FET02740
FET02750
FET02760
FET02770
FET02780
FET02790
FET02800
FET02810
FET02820
FET02830
FET02840
FET02850
FET02860
FET02870
FET02880
FET02890
FET02900
FET02910
FET02920
FET02930
FET02940
FET02950

C LATTER BOUNDARY CONTIONS TAKE PRECEDENCE OVER FORMER BOUNDARIES
 C
 C NOTE REVERSE READ Y1,Y2 THEN X1,X2...ETC IN READ(5,605)
 C XZ1,YZ1=X,Y COORDINATES OF TOP LEFT-HAND CCRNER OF BOUNDARY
 C XZ2=X COORDINATE OF RIGHT-HAND BOUNDARY.
 C YZ2=Y COORDINATE OF BOTTOM BOUNDARY.
 C UZ1,UZ2=LAMBDA,MU,RESPECTIVELY.
 C

20 READ(5,605) YZ1(N),YZ2(N),XZ1(N),XZ2(N),UZ1(N),UZ2(N)
 WRITE(6,606)N,XZ1(N),XZ2(N),YZ1(N),YZ2(N),UZ1(N),UZ2(N),N
 CONTINUE
 JJ=1

106 KCC=0
 DO 112 N=1,NBLKS,1
 KN=NBLK(N)
 GO TO(106,107,108,109,107),KN

107 KC=23
 GO TO 110
 108 KC=14
 GO TO 110
 109 KC=57
 GO TO 110

110 KCC=KCC+KC
 DO 801 I=1,NZ,1
 DO 111 J=JJ,KCC,1

E=XZ1(I)
 F=XZ2(I)
 G=YZ1(I)
 H=YZ2(I)
 IF(XC(J,1)).LT.E.OR.XC(J,2).LT.F.OR.XC(J,3).LT.G.OR.
 2 IF(XC(J,1)).GT.F.OR.XC(J,2).GT.G.OR.XC(J,3).GT.H) GO TO 111
 2 YC(J,1).GT.H.OR.YC(J,2).GT.H.OR.YC(J,3).GT.H) GO TO 111
 ELAM(J)=UZ1(I)*10.**ND
 EMU(J)=UZ2(I)*10.**ND

111 CONTINUE
 801 CONTINUE
 112 JJ=JJ+KC
 CONTINUE
 IF(IPO.GE.3)GO TO 113
 WRITE(6,724)
 WRITE(6,9034)

907 DO 113 J=1,K,1
 20 WRITE(6,9033) J,XC(J,1),YC(J,1),XC(J,2),YC(J,2),XC(J,3),YC(J,3),
 113 20(J),P(J),Q(J),ELAM(J),EMU(J),J
 CONTINUE
 IF (NF.EQ.0) GO TO 1113

C INPUT CARDS

FET02960
 FET02970
 FET02980
 FET02990
 FET03000
 FET03010
 FET03020
 FET03030
 FET03040
 FET03050
 FET03060
 FET03070
 FET03080
 FET03090
 FET03100
 FET03110
 FET03120
 FET03130
 FET03140
 FET03150
 FET03160
 FET03170
 FET03180
 FET03190
 FET03200
 FET03210
 FET03220
 FET03230
 FET03240
 FET03250
 FET03260
 FET03270
 FET03280
 FET03290
 FET03300
 FET03310
 FET03320
 FET03330
 FET03340
 FET03350
 FET03360
 FET03370
 FET03380
 FET03390
 FET03400
 FET03410
 FET03420
 FET03430
 FET03440
 FET03450

FET03460
FET03470
FET03480
FET03490
FET03500
FET03510
FET03520
FET03530
FET03540
FET03550
FET03560
FET03570
FET03580
FET03590
FET03600
FET03610
FET03620
FET03630
FET03640
FET03650
FET03660
FET03670
FET03680
FET03690
FET03700
FET03710
FET03720
FET03730
FET03740
FET03750
FET03760
FET03770
FET03780
FET03790
FET03800
FET03810
FET03820
FET03830
FET03840
FET03850
FET03860
FET03870
FET03880
FET03890
FET03900
FET03910
FET03920
FET03930
FET03940
FET03950

```

C
C
FY=NORMAL FORCE.
READ(5,707) (FY(I),I=1,NF)
DO 705 I=1,NCDE
  FX(I)=0
  IF(I+NF.GT.NODE) GO TO 5555
  FY(I+NF) = 0
5555 CONTINUE
  FY(I)=FY(I)*10.**NB
  NDISP(I)=0
  NDISP(I+NODE)=0
  DISP(I)=1
  DISP(I+NODE)=1
705 CONTINUE
  IF(KEND.EQ.0)GO TO 4445
  DO 60 J=1,9,1
    NBL=1
    IF(J.EQ.4.OR.J.EQ.6.OR.J.GE.8) GO TO 61
    IF(J.EQ.7) NBL=2
    LAY(J)=1
    DO 62 N=1,NBLKS,1
      K=NBLK(N)
      GO TO(63,64,65,66,64,66),K
      LAY(J)=LAY(J)+2
      GO TO 62
      LAY(J)=LAY(J)+1
      GO TO 62
      LAY(J)=LAY(J)+4
      GO TO 62
      LAY(J)=LAY(J)+8/NBL
      CONTINUE
      GO TO 60
    IF(J.GE.8)GO TO 67
    LAY(J)=0
    DO 68 N=1,NBLKS,1
      K=NBLK(N)
      GO TO(68,69,70,71,68,71),K
      LAY(J)=LAY(J)+1
      GO TO 68
      LAY(J)=LAY(J)+4
      GO TO 68
      LAY(J)=LAY(J)+8
      CONTINUE
      GO TO 60
    IF(J.EQ.9)GO TO 72
    LAY(J)=1
    DO 73 N=1,NBLKS,1
      K=NBLK(N)
      GO TO(74,75,74,74,75,74),K
      LAY(J)=LAY(J)+2

```



```

75 GO TO 73
73 LAY(J)=LAY(J)+1
CONTINUE
GO TO 60
72 LAY(J)=NBLKS+1
60 CONTINUE
IBL(1)=1
DO 76 J=2,9,1
IBL(J)=IEL(J-1)+1
IBL(J)=IEL(J-1)+LAY(J)
76 CONTINUE
IF(KBND.EQ.2) GO TO 4446
KBL=IBL(9)
KEL=IEL(9)
DO 4444 I=KBL,KEL,1
NDISP(I)=1
NDISP(I+NOD)=1
4444 CONTINUE
IF(KBND.EQ.1) GO TO 4445
DO 4445 I=1,8,1
IF(I.EQ.4.OR.I.EQ.6)GO TO 4445
NDISP(1BL(I))=1
NDISP(1EL(I))=1
NDISP(1BL(I)+NOD)=1
NDISP(1EL(I)+NOD)=1
4445 CONTINUE
NOD=0
IF(IPO.GE.6) GO TO 440
IF(IPO.EQ.1.OR.IPO.EQ.2)NOD=NOD=
IF(IPO.GE.3.AND.IPO.LE.5)NOD=NF
WRITE(6,725)
80 DO 708 I=1,NOD,1
WRITE(6,709) I,XF(I),YF(I),FX(I),FY(I),NDISP(I),DISP(I),
440 2NDISP(I+NOD),DISP(I+NOD),I
CONTINUE
708 CALL ASAPS(JOB)
1000 CONTINUE
GO TO 14
1111 WRITE(6,11)
1112 GO TO 14
1112 WRITE(6,12)
1113 GO TO 14
14 WRITE(6,13)
STOP
END

```

```

FET03960
FET03970
FET03980
FET03990
FET04000
FET04010
FET04020
FET04030
FET04040
FET04050
FET04060
FET04070
FET04080
FET04090
FET04100
FET04110
FET04120
FET04130
FET04140
FET04150
FET04160
FET04170
FET04180
FET04190
FET04200
FET04210
FET04220
FET04230
FET04240
FET04250
FET04260
FET04270
FET04280
FET04290
FET04300
FET04310
FET04320
FET04330
FET04340
FET04350
FET04360
FET04370
FET04380
FET04390
FET04400
FET04410
FET04420

```


SUBROUTINE ASAPS (NJ)

* FINITE ELEMENT METHOD FOR AXISYMMETRIC*
* AND PLANE-STRAIN PROBLEMS*

```

      CCMON G(750),P(750),Q(750),XC(750,3),YC(750,3),
      2X (425),Y(425),FX(425),FY(425),NDISP(0850),DISP(0850),
      3 XZ1(025),XZ2(025),YZ1(025),YZ2(025),UZ1(025),UZ2(025),
      4 A(850,16),AREN(750),AR(850),B(850),ELAM(750),EMU(750),
      5 LIDS(425,7),LID(425,8,2),MAP(850,16),MID(425,8),
      6 NA,NB,NC,ND,NODE,NCELL,IGEOM,ITERAT,W,NF,IPO
      DIMENSION XPLUT(100),DIST(5)
      INTEGER O,P,Q,ON,PN,QN,OTEMP,GE,PE,QE
      13 FORMAT(6X,I3,2F10.5)
      110 FORMAT(18X,13HDISPLACEMENTS)
      111 FORMAT(4X,4HNODE,7X,6HX-COMP,9X,6HY-COMP,9X,7HX-COORD,8X,
      17HY-COORD,/)
      113 FORMAT(5X,I3,4X,E11.4,X,E11.4,2E12.4)
      163 FORMAT(1H1,1X,1ITERATION,I4)
      830 FORMAT(5X,59HBLW UP OF XUN IN SOLUTION OF EQUATIONS ...POSSIBLE
      1RROR IN X Y DATA)
      831 FORMAT(5X,19HNODE X(I) Y(I))

```

```

      LINES=1
      MIS=NF/6
      MIDD=MIS+NODE
      CUT=0.000001
      LPLOT=NF
      FILL=100.
      ITHR=0
      NPT=IPO
      RNG=0.
      DMIN=0.
      DAY1=1.
      IT=2*NODE
      DO 51 I=1,NODE,1
      DO 51 J=1,7,1
      DO 52 J=1,7,1
      LIDS(I,J)=0
      52 CONTINUE
      DO 53 J=1,8,1
      MID(I,J)=0
      DO 54 K=1,2,1
      LID(I,J,K)=0
      54 CONTINUE
      53 CONTINUE
      51 CONTINUE
      MID(I,J)=NATURALLY OCCURRING NODE PAIRS...MID(I,K)=J I,J=NODES
      K=1-8

```

LIDS(I,J)=ALL CELLS WITH NODE I...J=1-7

FET04440
FET04450
FET04460
FET04470
FET04480
FET04490
FET04500
FET04510
FET04520
FET04530
FET04540
FET04550
FET04560
FET04570
FET04580
FET04590
FET04600
FET04610
FET04620
FET04630
FET04640
FET04650
FET04660
FET04670
FET04680
FET04690
FET04700
FET04710
FET04720
FET04730
FET04740
FET04750
FET04760
FET04770
FET04780
FET04790
FET04800
FET04810
FET04820
FET04830
FET04840
FET04850
FET04860
FET04870
FET04880
FET04890
FET04900
FET04910
FET04920
FET04930


```

C
C
      LID(I,J,K)=CELLS WITH NODE PAIR I,L...L=MID(I,J),K=1-2
      DO 60 I=1,NODE,I
      MID(I,I)=I
      CONTINUE
60  DO 61 I=1,NCELL,I
      QN=Q(I)
      PN=P(I)
      CN=C(I)
      DO 62 IC=1,3,I
      IF(IC.EQ.1) JT=QN
      IF(IC.EQ.2) JT=PN
      IF(IC.EQ.3) JT=CN
      DO 55 J=1,7,I
      IF(LIDS(JT,J).EQ.0) GO TO 63
999 IF(LIDS(JT,J).EQ.0) GO TO 63
      CONTINUE
55  WRITE(6,833)JT
      WRITE(6,834)
      WRITE(6,835)(LIDS(JT,IE),IE=1,7,1),I
      STOP
833 FORMAT(3X,39HERROR...TOO MANY CELLS ADJACENT TO NODE,I3)
834 FORMAT(3X,26HCELLS ADJACENT TO THE NODE)
835 FORMAT(3X,8I6)
63  LIDS(JI,J)=I
      J=J+1
62  CONTINUE
      DO 64 ITP=1,3,I
      DO 73 J=2,8,I
      IF(MID(ON,J).EQ.0) GO TO 66
      IF(MID(ON,J).EQ.PN) GO TO 67
73  CONTINUE
66  MID(ON,J)=PN
      J=J+1
67  DO 74 J=2,8,I
      IF(MID(ON,J).EQ.0) GO TO 68
      IF(MID(ON,J).EQ.QN) GO TO 69
74  CONTINUE
      IF(J.EQ.9) WRITE(6,850) ON,(MID(ON,K),K=2,8,1),QN
      IF(J.EQ.9) STOP
850 FORMAT(2X,20HERROR IN DATA, NODE ,I3,2X,20HADJACENT TO NODES
15)
68  MID(ON,J)=QN
      J=J+1
69  OTEMP=QN
      CN=PN
      PN=QN
      QN=OTEMP
      CONTINUE
64  DO 70 I=1,NODE,I
61

```

FET049940
 FET049950
 FET049960
 FET049970
 FET049980
 FET049990
 FET050000
 FET050010
 FET050020
 FET050030
 FET050040
 FET050050
 FET050060
 FET050070
 FET050080
 FET050090
 FET050100
 FET050110
 FET050120
 FET050130
 FET050140
 FET050150
 FET050160
 FET050170
 FET050180
 FET050190
 FET050200
 FET050210
 FET050220
 FET050230
 FET050240
 FET050250
 FET050260
 FET050270
 FET050280
 FET050290
 FET050300
 FET050310
 FET050320
 FET050330
 FET050340
 FET050350
 FET050360
 FET050370
 FET050380
 FET050390
 FET050400
 FET050410
 FET050420
 FET050430

FET05440
FET05450
FET05460
FET05470
FET05480
FET05490
FET05500
FET05510
FET05520
FET05530
FET05540
FET05550
FET05560
FET05570
FET05580
FET05590
FET05600
FET05610
FET05620
FET05630
FET05640
FET05650
FET05660
FET05670
FET05680
FET05690
FET05700
FET05710
FET05720
FET05730
FET05740
FET05750
FET05760
FET05770
FET05780
FET05790
FET05800
FET05810
FET05820
FET05830
FET05840
FET05850
FET05860
FET05870
FET05880
FET05890
FET05900
FET05910
FET05920
FET05930

```

71 J=2,8,1
LTEMP=MID(I,J)
IF(LTEMP.EQ.0)GO TO 70
C0 72 K=1,7,1
KTEMP=LIDS(I,K)
IF(KTEMP.EQ.0) GO TO 71
CN=O(KTEMP)
PN=P(KTEMP)
CN=Q(KTEMP)
M=1
IF(LID(I,J,M).NE.O) M=2
IF(CN.EQ.LTEMP.OR.PN.EQ.LTEMP.OR.QN.EQ.LTEMP)LID(I,J,M)=KTEMP
CONTINUE
CONTINUE
CONTINUE
72 LET A(I,J)=0,MAP(I,J)=0,B(I)=0
71 DO 77 I = 1, I1
70 DO 78 J = 1, 16, 1
C
  A(I,J)=0
  MAP(I,J)=0
  CONTINUE
78 B(I)=0
77 CONTINUE
  ITERATION ON I=NCELL IS TO FORM YC(..),XC(..)
  DO 85 I = 1, NCELL, 1
  QN=O(I)
  PN=P(I)
  QN=Q(I)
  YC(I,1)=Y(PN)-Y(QN)
  YC(I,2)=Y(QN)-Y(QN)
  YC(I,3)=Y(QN)-Y(PN)
  XC(I,1)=X(QN)-X(PN)
  XC(I,2)=X(QN)-X(QN)
  XC(I,3)=X(PN)-X(QN)
  AREN(I)=.5*(XC(I,1)*YC(I,3)-XC(I,3)*YC(I,1))
  CONTINUE
85
C
  *****
  * FORM STIFFNESS MATRIX *
  *****
  DO 90 I=1,NODE,1
  IV=NODE+I
  DO 91 JA=1,8,1
  J=MID(I,JA)
  JB=JA+8
  LD=0
  DO 92 KA=1,7,1
  LD=LD+1
  IF(I.EQ.J) GO TO 94

```



```

C
DO 100 I=1,NODE,1
IV=NODE+I
B(I)=FX(I)
B(IV)=FY(I)
CONTINUE
100 ARRANGE MATRIX FOR SOLUTION
DO 101 I=1,IT,1
DO 102 J=1,16,1
IF (I.EQ. MAP(I,J)) GO TO 103
CONTINUE
102 AR(I)=A(I,J)
103 CONTINUE
101

C
C SOLVE SIMULTANEOUS EQUATIONS
M=0
DO 104 L=1,ITERAT,1
DO 105 I=1,IT,1
IF (NDISP(I).EQ.1) GO TO 105
TEMP=0.
DO 106 J=1,16,1
IF (MAP(I,J).EQ.0) GO TO 106
IF (I.EQ. MAP(I,J)) GO TO 106
JROW=MAP(I,J)
TEMP=TEMP+A(I,J)*DISP(JROW)
CONTINUE
106 DISP(I) = ((B(I)-TEMP)/AR(I))*W+((1.-W)*DISP(I))*10.**NC
IF (DISP(I).GT.1.0E07) GO TO 825
CONTINUE
105 IF (L.NE.25.AND.L.LE.49) GO TO 104
IF (L=25) ITL=25*ITL
IF (ITL.NE.L) GO TO 901
M=M+1
GO TO (15,16,2001),M
DIST(M)=SQRT((DISP(MIS))**2+(DISP(MIDD))**2)
DO 1010 I=1,104
DIST(N)=SQRT((DISP(MIS))**2+(DISP(MIDD))**2)
PERC=SQRT((DIST(M-1)-DIST(M))**2)/DIST(M-1)
DIST(M-1)=DIST(M)
M=M-1
IF (PERC.LE.CUT) GO TO 902
CONTINUE
104 M=2
902 WRITE(6,163) L
904 IF (IPO.EQ.8) GO TO 2
WRITE(6,110)
WRITE(6,111)
NOD=NODE
2

```



```

VP=DISP(PE)
VQ=DISP(QE)
EX={UO*YC(I,1)+UP*YC(I,2)+UQ*YC(I,3)}/{2.*AREN(I)}
EY={VO*XC(I,1)+VP*XC(I,2)+VQ*XC(I,3)}/{2.*AREN(I)}
EY=(UO*XC(I,1)+UP*XC(I,2)+UQ*XC(I,3)+VO*YC(I,1)+VP*YC(I,2)+VQ*YC(I,3))/(4.*AREN(I))
AE=EX-EY
BE=EX+EY
AEP=ABS(AE)
IF(AEP.LT..00001) GO TO 201
EBETA=ATAN(2.*EY)/AE)/2.
GO TO 202
201 EBETA=3.14159/4.
202 EGAM=EBETA+3.14159/2.*COS(2.*EBETA)+EY*SIN(2.*EBETA)
EPI=(BE/2.)+(AE/2.)*COS(2.*EGAM)+EY*SIN(2.*EGAM)
EP2=(BE/2.)+(AE/2.)*COS(2.*EGAM)+EY*SIN(2.*EGAM)
IF(EPI.LT.EP2) GO TO 203
EMAX=EPI
EMIN=EP2
THETA1=EBETA
THETA2=EGAM
GO TO 204
203 EMAX=EP2
EMIN=EPI
THETA1=EGAM
THETA2=EBETA
GO TO 205
204 DELV=(EMAX+EMIN)/2.
SIGMAX=2.*EMU(I)*EMAX+ELAM(I)*2.*DELV
SIGMIN=2.*EMU(I)*EMIN+ELAM(I)*2.*DELV
PRESS=(SIGMAX+SIGMIN)/2.
SHEAR=(SIGMAX-SIGMIN)/2.
HOOPE=0.
HOOPS=0.
IF(IGEOM.EQ.1) GO TO 205
QE=QE-NODE
PE=PE-NODE
QE=QE-NODE
HOOPE=UO+UP+UQ)/(X(QE)+X(PE)+X(QE))
DELV=(HOOPE+EMAX+EMIN)/3.
SIGMAX=2.*EMU(I)*EMAX+ELAM(I)*3.*DELV
SIGMIN=2.*EMU(I)*EMIN+ELAM(I)*3.*DELV
PRESS=2.*SIGMAX+HOOPE)/3.
HOOPS=2.*EMU(I)*HOOPE+ELAM(I)*3.*DELV
IF(HOOPS.LT.SIGMAX.AND.HOOPS.GT.SIGMIN) SHEAR=(SIGMAX-SIGMIN)/2.
IF(HOOPS.LT.SIGMAX) SHEAR=(HOOPS-SIGMIN)/2.
IF(HOOPS.LT.SIGMIN) SHEAR=(SIGMAX-HOOPS)/2.
WRITE(6,214)I,SIGMAX,SIGMIN,EMAX,EMIN,THETA1,THETA2,HOOPS,HOOPE,
1SHEAR,PRESS

```

FET07440
FET07450
FET07460
FET07470
FET07480
FET07490
FET07500
FET07510
FET07520
FET07530
FET07540
FET07550
FET07560
FET07570
FET07580
FET07590
FET07600
FET07610
FET07620
FET07630
FET07640
FET07650
FET07660
FET07670
FET07680
FET07690
FET07700
FET07710
FET07720
FET07730
FET07740
FET07750
FET07760
FET07770
FET07780
FET07790
FET07800
FET07810
FET07820
FET07830
FET07840
FET07850
FET07860
FET07870
FET07880
FET07890
FET07900
FET07910
FET07920
FET07930


```

214 13X,FORMAT(2X,I3,I3,3X,E11.4,2X,E11.4,2X,E11.4,1X,E11.4,1X,F7.2,2X,F7.2,
      13X,E11.4,2X,E11.4,3X,E11.4,4X,E11.4)
      SIGX=2.*EMU(I)*EX+ELAM(I)*(EX+EY)
      SIGY=2.*EMU(I)*EY+ELAM(I)*(EX+EY)
      SIGXY=2.*EMU(I)*EXY
      WRITE(6,950) SIGX,SIGY,SIGXY
950  FORMAT(12X,E11.4,2X,E11.4,2X,E11.4)
200  CONTINUE
2001 CONTINUE
      RETURN
      END
FET07940
FET07950
FET07960
FET07970
FET07980
FET07990
FET08000
FET08010
FET08020
FET08030
FET08040

```


FET08560
FET08570
FET08580
FET08590

WRITE(6,205)
FORMAT(1H1)
RETURN
END

205

FOLLOWING IS BLOCK DATA ARRAY. IT IS ALWAYS THE FIRST FIFTEEN
CARDS IN DATA DECK. BLOCK ARRAY ALWAYS REMAINS THE SAME REGARDLESS
OF THE NUMBER OR TYPE OF MODELS TO BE PROCESSED.
THE FORMAT OF THE BLOCK ARRAY IS 10F5.1

2.0	0.2	2.1	0.0	2.2	0.0	2.3	0.0	2.4	0.0	0.0	0.0	0.0	0.0	4.0	1
1.0	1.0	1.0	1.0	1.0	1.0	1.0	1.0	1.0	1.0	0.0	0.0	0.0	0.0	0.0	2
1.0	0.2	1.0	1.0	1.0	1.0	1.0	1.0	1.0	1.0	0.0	0.0	0.0	0.0	1.0	3
1.0	1.0	1.0	1.0	1.0	1.0	1.0	1.0	1.0	1.0	0.0	0.0	0.0	0.0	0.0	4
0.2	0.2	1.0	1.0	1.0	1.0	1.0	1.0	1.0	1.0	0.0	0.0	0.0	0.0	2.0	5
0.2	0.2	1.0	1.0	1.0	1.0	1.0	1.0	1.0	1.0	0.0	0.0	0.0	0.0	0.0	6
0.5	0.5	1.0	1.0	1.0	1.0	1.0	1.0	1.0	1.0	0.0	0.0	0.0	0.0	0.0	7
0.2	0.2	1.0	1.0	1.0	1.0	1.0	1.0	1.0	1.0	0.0	0.0	0.0	0.0	0.0	8
0.5	0.5	1.0	1.0	1.0	1.0	1.0	1.0	1.0	1.0	0.0	0.0	0.0	0.0	0.0	9
0.2	0.2	1.0	1.0	1.0	1.0	1.0	1.0	1.0	1.0	0.0	0.0	0.0	0.0	0.0	10
0.2	0.2	1.0	1.0	1.0	1.0	1.0	1.0	1.0	1.0	0.0	0.0	0.0	0.0	0.0	11
0.2	0.2	1.0	1.0	1.0	1.0	1.0	1.0	1.0	1.0	0.0	0.0	0.0	0.0	0.0	12
0.2	0.2	1.0	1.0	1.0	1.0	1.0	1.0	1.0	1.0	0.0	0.0	0.0	0.0	0.0	13
0.2	0.2	1.0	1.0	1.0	1.0	1.0	1.0	1.0	1.0	0.0	0.0	0.0	0.0	0.0	14
0.2	0.2	1.0	1.0	1.0	1.0	1.0	1.0	1.0	1.0	0.0	0.0	0.0	0.0	0.0	15

BIBLIOGRAPHY

1. Carey, G.F. and Martin, H.C., Introduction to Finite Element Analysis, McGraw-Hill, 1973.
2. Crowley, F.A., Ossing, H.A. and Cabiness, G.H., Precursory Siloed Missile Geokinetic Study Hill, Air Force Base, Utah, Air Force Surveys in Geophysics, Vol. 245, Sep 1972.
3. Dieterich, J.H., Documentation ASAPS Subroutine, National Center for Earthquake Research Program Library, Sep 1970.
4. Fix, G.J. and Strang, G., An Analysis of the Finite Element Method, Prentice-Hall, 1973.
5. Froberg, C.E., Introduction to Numerical Analysis, Addison-Wesley, 1965.
6. Grant, F.S. and West, G.F., Interpretation Theory In Applied Geophysics, McGraw Hill, 1965.
7. Mayer-Rosa, D., Travel-Time Anomalies and Distribution of Earthquakes Along the Calveras Fault Zone, California, Bulletin of the Seismological Society of America, Vol. 63, pp. 713-729, April 1973.
8. Melchior, P., The Earth Tides, Pergamon Press, 1966.
9. Smith, G.N., An Introduction to Matrix and Finite Element Methods in Civil Engineering, Applied Science Publishers, 1971.
10. Smith, P.J., Topics In Geophysics, The MIT Press, 1973.
11. Stewart, S.W., Preliminary Comparison of Seismic Travel Times and Inferred Crustal Structures Adjacent to the Diablo and Gablin Ranges of Central California, Stanford University Publications in the Geological Sciences, Vol. 11, pp. 218-230, 1968.
12. Wood, M.D., The Influence of Ocean Tidal Loading on Solid Earth Tides and Tilts in the San Francisco Bay Region, California, Ph.D. Thesis, Stanford University, 1969.
13. Wood, M.D., Allen, R.V. and Allen, S.S., Methods for Prediction and Evaluation of Tidal Tilt Data from Borehole and Observatory Sites Near Active Faults, Phil. Trans. R. Soc., London, Vol. 274, pp. 245-252, 1973.

14. Tide Harmonic Constants, International Hydrographic Bureau, Monaco, July 1953.
15. Zienkiewicz, O.C. and Cheung, Y.K., The Finite Element Method In Structural and Continuum Mechanics, McGraw-Hill, 1967.

INITIAL DISTRIBUTION LIST

	No. Copies
1. Defense Documentation Center Cameron Station Alexandria, Virginia 22314	2
2. Library, Code 0212 Naval Postgraduate School Monterey, California 93940	2
3. Department Chairman, Code 55 Department of Operations Research and Administrative Sciences Naval Postgraduate School Monterey, California 93940	2
4. Associate Professor Donald R. Barr, Code 55 Bn Department of Operations Research and Administrative Sciences	1
5. Associate Professor Rex H. Shudde, Code 55 Su Department of Operations Research and Administrative Sciences Naval Postgraduate School Monterey, California 93940	1
6. Captain Robert C. Foos 13060 Luber Street Salinas, California 93901	1
7. U.S. Army Military Personnel Center Attn: DAPC-OPD-PD-CS 200 Stovall Street Alexandria, Va. 22232	1
8. Chief of Naval Personnel Attn: Pers 11b Department of the Navy Washington, DC 20370	1
9. Dr. M. Darroll Wood National Center for Earthquake Research 800 Menlo Ave. Menlo Park, Ca. 94025	1



Thesis
F5767 Foos
c.1

160101

Modeling an input-
output geokinetic
system utilizing a
finite element approach.

Thesis
F5767 Foos
c.1

160101

Modeling an input-
output geckinetic
system utilizing a
finite element approach.

thesF5767

Modeling an input-output geokinetic syst



3 2768 000 99905 6

DUDLEY KNOX LIBRARY